UNIVERSITÀ DI PARMA
ARCHIVIO DELLA RICERCA

University of Parma Research Repository

Hypogenic origin, geologic controls and functional organization of a giant cave system in Precambrian carbonates, Brazil

note finali coverpage

(Article begins on next page)

06 February 2025

Accepted Manuscript

Hypogenic origin, geologic controls and functional organization of a giant cave system in Precambrian carbonates, Brazil

Alexander Klimchouk, Augusto S. Auler, Francisco H.R. Bezerra, Caroline L. Cazarin, Fabrizio Balsamo, Yuri Dublyansky

Please cite this article as: Klimchouk, Alexander, Auler, Augusto S., Bezerra, Francisco H.R., Cazarin, Caroline L., Balsamo, Fabrizio, Dublyansky, Yuri, Hypogenic origin, geologic controls and functional organization of a giant cave system in Precambrian carbonates, Brazil, *Geomorphology* (2015), doi: 10.1016/j.geomorph.2015.11.002

Geomorphology (2016), vol. 253, pp. 385-405

This is a PDF file of an unedited manuscript that has been accepted for publication. As a service to our customers we are providing this early version of the manuscript. The manuscript will undergo copyediting, typesetting, and review of the resulting proof before it is published in its final form. Please note that during the production process errors may be discovered which could affect the content, and all legal disclaimers that apply to the journal pertain.
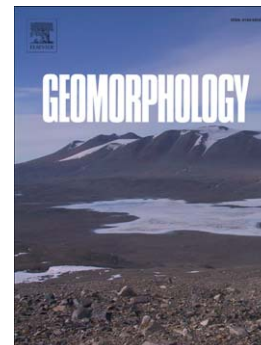
Hypogenic origin, geologic controls and functional organization of a giant cave system in Precambrian carbonates, Brazil

Alexander Klimchouk[1]*, Augusto S. Auler[2], Francisco H.R. Bezerra[3], Caroline L. Cazarin[4], Fabrizio Balsamo[5], Yuri Dublyansky[6]

[1]Institute of Geological Sciences, National Academy of Science, Ukraine
[2]Instituto do Carste, Brazil
[3]Department of Geology, Federal University of Rio Grande do Norte, Brazil
[4]Petrobras, Centro de Pesquisa e Desenvolvimento Leopoldo A. Miguez de Mello, Brazil
[5]NEXT - Natural and Experimental Tectonic Research Group, Department of Physic and Earth Sciences, University of Parma, Italy
[6]Institute of Geology, Innsbruck University, Austria

Corresponding author: klim@speleogenesis.info, phone: +380503522948

Abstract

This study is focused on speleogenesis of the Toca da Boa Vista (TBV) and Toca da Barriguda (TBR), the longest caves in South America occurring in the Neoproterozoic Salitre Formation in the São Francisco Craton, NE Brazil. We employ a multidisciplinary approach integrating detailed speleomorphogenetic, lithostratigraphic and geological structure studies in order to reveal the origin of the caves, their functional organization and geologic controls on their development. The caves developed in deep-seated confined conditions by rising flow. The overall fields of passages of TBV and TBR caves represent a speleogenetically exploited large NE-SW-trending fracture corridor associated with a major thrust. This corridor vertically extends across the Salitre Formation allowing the rise of deep fluids. In the overall ascending flow system, the formation of the cave pattern was controlled by a system of sub-parallel anticlines and troughs with NNE-SSW dominant orientation, and by vertical and lateral heterogeneities in fracture distribution. Three cave-stratigraphic storeys reflect the actual hydrostratigraphy during the main phase of speleogenesis. Cavities at different storeys are distinct in morphology and functioning. The gross tree-dimensional pattern of the system is effectively organized to conduct rising flow in deep-seated confined conditions. Cavities in the lower storey developed as recharge components to the system. A laterally extensive conduit network in the middle storey formed because the vertical flow from numerous recharge points has been redirected laterally along the highly conductive unit, occurring below the major seal – a scarcely fractured unit. Rift-like and shaft-like conduits in the upper storey developed along fracture-controlled outflow paths, breaching the integrity of the major seal, and served as outlets for the cave system. The cave system represents a series of vertically organized, functionally largely independent clusters of cavities

1

developed within individual ascending flow cells. Lateral integration of clusters occurred due to hydrodynamic interaction between the flow cells in course of speleogenetic evolution and change of boundary conditions. The main speleogenetic phase, during which the gross cave pattern has been established and the caves acquired most of their volume, was likely related to rise of deep fluids at about 520 Ma or associated with rifting and the Pangea break-up in Triassic – Cretaceous. This study highlights the importance of speleogenetic studies for interpreting porosity and permeability features in carbonate reservoirs.

Key words: hypogenic speleogenesis, Salitre Formation, São Francisco Craton, NE Brazil.

1 Introduction

Historically, karst studies were mainly concerned with shallow, hydrogeologically unconfined settings where karstification is related to direct recharge from the overlying surface (i.e., epigene karst). For a long time, the possibility of deep-seated karst development (hypogene karst) was deemed to be low to nonexistent within the dominant "geomorphological" paradigm of karst. Solution porosity features found in deep burial environments have commonly been interpreted as paleo-(epigenic) karst, i.e. karst that had commenced in exposed settings but later buried under younger strata.

The last decade has witnessed an expansion in the recognition of importance of hypogene karst (speleogenesis) that develops by upwelling flow, without direct genetic relationship to the surface. Previously regarded as an aberrant phenomenon of local significance, hypogene karst is now increasingly recognized as one of the fundamental categories of karst of wide global occurrence and importance (Klimchouk, 2007, 2009, 2012). At the same time, it has become clear that speleogenesis, and resultant patterns and functioning of void-conduit systems, differ fundamentally between hydrogeologically confined deep-seated, hypogene settings and surface-related epigene settings. Thus, the identification of the cave origin (type of speleogenesis) is of paramount importance for many practical fields concerned with post-depositional heterogeneities and fluid flow in soluble rocks. This is particularly true for carbonate reservoir characterization as they host around 60 % of the world's oil and 40 % of the world's gas (Montaron, 2008), including many super-giant and highly productive fields. Meanwhile, prospecting and exploitation of such reservoirs presents many difficult challenges stemming from poor understanding of the properties of karst void-conduit systems. Being the result of fluid circulation in a given geological media comprising soluble rocks, solutional void-conduit systems contain a wealth of information about fluid history and geological (geodynamic, hydrogeological, geomorphological, etc.) evolution of an area. When evolved, such systems exert a dominant control over subsurface fluid flow. Detailed studies of large accessible cave systems are indispensable for improving our understanding of speleogenetic processes and, therefore, of resultant porosity and permeability in carbonate reservoirs. Such cave systems can serve as analogues of karst reservoirs.

With current advances in studying hypogenic speleogenesis, the origin of caves in many regions is being re-interpreted (e.g. Klimchouk and Ford, 2009; Stafford et al., 2009). The diversity of hypogene cave patterns is now recognized as the result of complex interplay of geological conditions and cave-

forming processes, varying in space and time (Klimchouk, 2007; Audra, 2009b). However, geologic controls over fluid flow and speleogenesis in hypogene settings are not yet sufficiently understood.

This study is focused on speleogenesis of the cave system consisting of the Toca da Boa Vista (TBV) and Toca da Barriguda (TBR) caves. These caves, occurring in the Neoproterozoic carbonates of the Salitre Formation (Una Group) in the São Francisco Craton, Brazil (Fig. 1), are the longest in South America and among the longest in the Southern Hemisphere, with mapped conduit lengths of ca. 107 and ca. 34 km respectively. Early studies of the caves (Auler, 1999; Auler and Smart, 2003) recognized their hypogene character but proposed a model of shallow speleogenesis in a laterally flowing aquifer. Here we present a multidisciplinary approach integrating detailed speleomorphogenetic studies and studies of lithostratigraphy and geological structure (fracturing and folding), which allowed us (1) to demonstrate the origin of the caves by deep ascending flow under confined conditions, (2) unravel the functional organization of the cave system, and (3) constrain geological controls over the cave development.
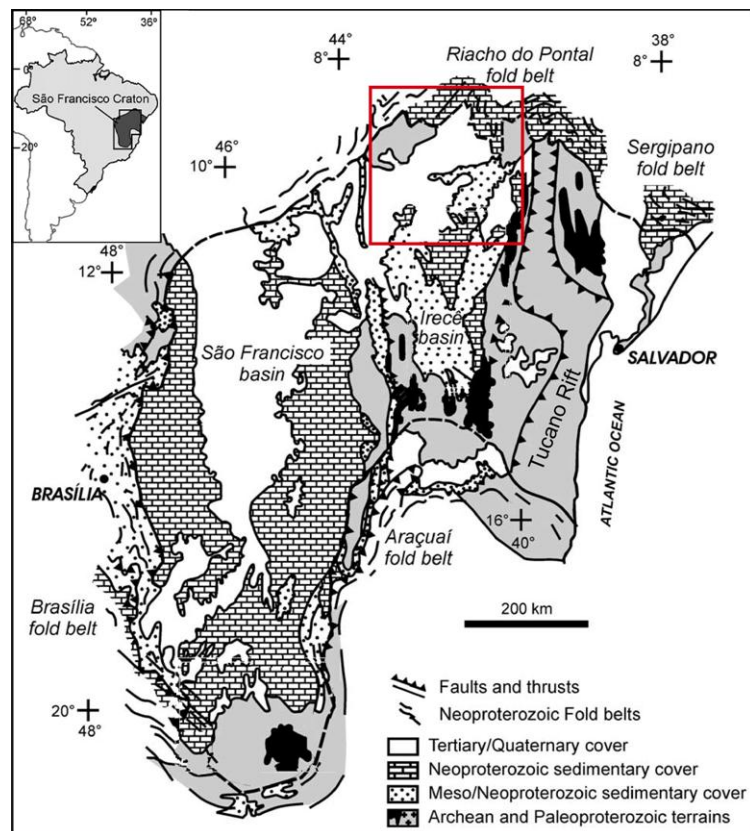

Figure 1. Geological map of the São Francisco Craton showing Neoproterozoic basins, surrounding fold belts, and the study area (red square cf. Fig. 2 A). From Santos et al. (2000), as modified by Trindade et al. (2004).

2 The study area

TBV and TBR are located close to the village of Laje dos Negros in the municipality of Campo Formoso (Bahia State), in the northeastern Brazil (Fig. 1). The study area is in the northern part of the São Francisco Craton (Fig. 2) that has been preserved from the Brasiliano orogeny at 740-580 Ma, although this part of the craton was influenced by deformations in the Riacho do Pontal belt to the north (Brito Neves et al., 2014). The caves develop in the carbonate Salitre Formation, a part of the Una Group comprised by marine limestones and dolomites. The Salitre Formation (700-560 Ma) and its correlative units in the Bambui Group have been a part of an extensive Neoproterozoic platform, with sedimentation commencing during transgression of an epicontinental sea over much of the São Francisco Craton and surrounding areas (Misi and Kyle, 1994). According to Misi (1993) the thickness of the Salitre Formation varies through the region from 550 m to 1000 m, but in the cave area it does not seem to exceed 200 m.
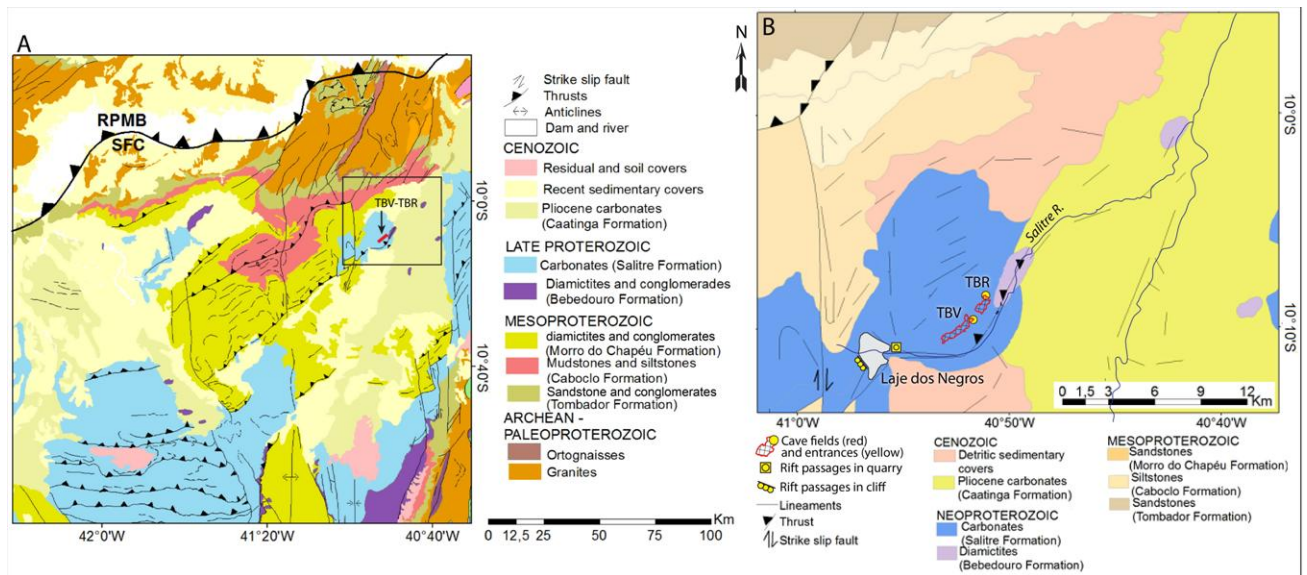
Figure 2. A - geological map of the northern part of the São Francisco Craton showing major lithostratigraphic units and tectonic structures (simplified from Bizzi et al., 2003). Location of the TBV-TBR system is indicated by a small bar pointed to by the arrow. B - geological map of study area and location of the TBV-TBR caves and the quarry and the cliff with rift-like passages.

The landscape of the area is a monotonous plain with subdued hills. Both caves are located (TBV - 10º09'45"S, 40º51'35"W; TBR - 10º08'26"S, 40º51'08"W) on the left bank of the ephemeral Salitre

River. The cave fields (the areas of integrated passage development) form a belt trending NE-SW (Fig. 2). In addition, rift-like cave passages forming a small reticular maze are located in the slope of a hill at the NE edge of the village, where they are truncated by the denudation surface and partly destroyed by a small quarry. Similar rift-like passages at approximately the same altitude and stratigraphic position, open in a cliff that stretches along the south-west edge of the village on the opposite side of the river, but they do not extend far into the massif. They show phreatic morphology with cupolas in the ceilings.

The Salitre Formation rocks form the surface throughout the cave area. Some 3-4 km east of the caves they are overlain by the Caatinga freshwater limestones, extending as a wide cover along the Salitre River. The limestones of varied degrees of consolidation, from soft chalky to crystalline indurated rocks, with a thickness of 20 m on average (locally up to 80 m), were deposited in palustrine environment in late Pliocene or early Pleistocene (Penha, 1994; Auler, 1999).

There are no direct data from the cave area on the geometry and depth of occurrence of the lower contact of the Salitre Formation. Across the broader region, the Salitre Formation is underlain mainly by diamictites and arkoses of the basal glaciogenic unit, the Bebedouro Formation, and by older sandstones, metapellites and other sedimentary rocks of the Chapada Diamantina and Espinhaco groups (Mesoproterozoic). The Bebedouro Formation is exposed in a ridge located some 10 km to the NW of the caves, and can be observed below the Caatinga limestones in the Salitre River valley 14-16 km NE of the caves. Also, Archaean schists are exposed in places within the Rio Salitre drainage channel. The thickness of the Salitre Formation in the cave area can be estimated to be at least 80-100 m, but likely it does not exceed 200 m.

The Campo Formoso area has a semi-arid climate with rainfall of around 490 mm per year. Despite of extensive exposure of the Salitre carbonates in the area, surface karst landforms are poorly developed, being represented mainly by small-scale solution features (karren) and rare dolines of collapse origin. Auler and Smart (2003) stressed the remarkable contrast between the subdued surface karst development and the extensive development of the spectacular underground features, an indication that the latter have no genetic relation with the landscape.

3 Previous views on speleogenesis of the TBV-TBR cave system

TBV and TBR were explored and surveyed by the Grupo Bambui de Pesquisas Espeleologicas (Bambuí Group of Speleological Research), beginning in the late 1980s. These efforts resulted in the basic maps of the caves used in our analysis, a simplified outline version of which is shown in Fig. 3.
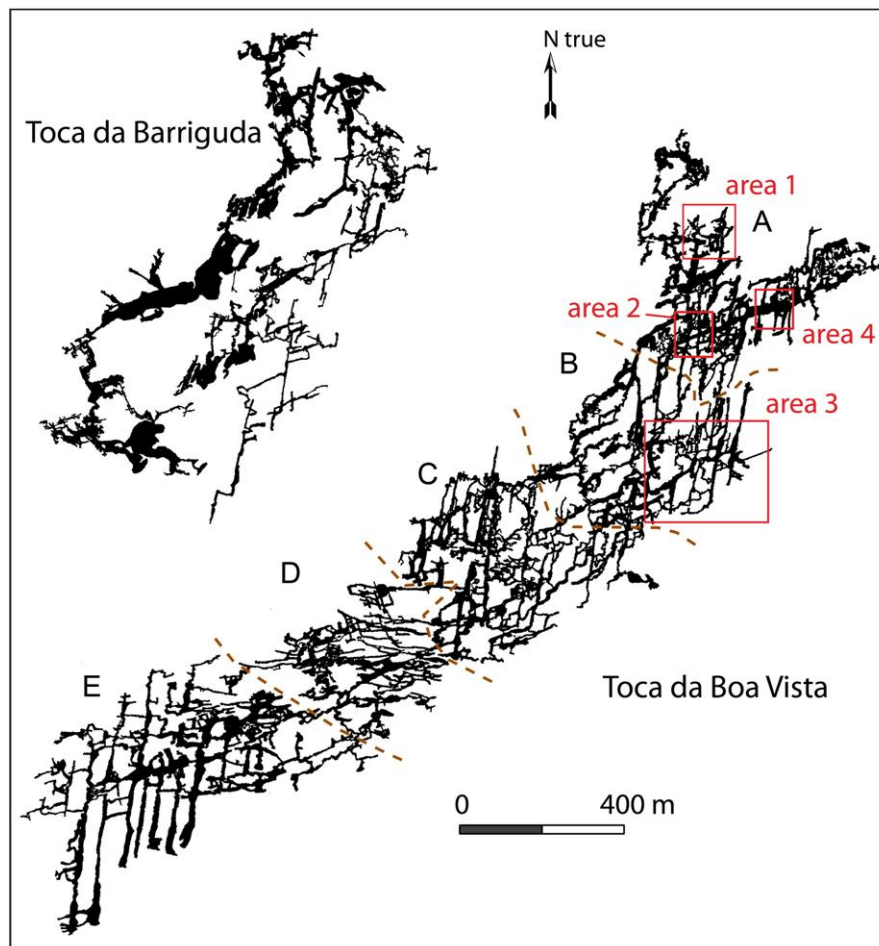
Figure 3. Outline maps of Toca da Boa Vista and Toca da Barriguda. The caves are not in their true relative position (cf. Fig. 2 B). Maps are a courtesy of Bambuí Group of Speleological Research. Dashed lines delineate sectors in TBV with distinct passage patterns (A-E). Rectangles show areas were detailed morphogenetic mapping was carried out.

Speleogenesis of the TBV-TBR system has been addressed by Auler and Smart (2003), who concluded that the morphology of the caves conform to the general character of hypogenic caves, suggesting that climate-controlled processes were not a determinant in the speleogenesis in the area. They stressed several features of TBV and TBR which are characteristic of hypogene speleogenesis, including: lack of genetic relationship with the surface terrain and scarcity of karst landforms in the area; mixed network/ramiform pattern of the caves; lack of discharge control of passage morphology and size; abrupt variations in passage cross-sections over short distances; absence of fluvial sediments and vadose speleogens. At the same time, Auler and Smart (2003) thought that the caves lacked three-dimensional architecture and morphological evidence of rising flow diagnostic of the deep-

seated hypogene speleogenesis. Also, the local geology was thought not to favor deep-seated hypogenic speleogenesis because the Salitre Formation is underlain by either quartzite or schist and the area is located in a stable craton in which no tectonic activity was assumed to have occurred since the beginning of the Cambrian. It was proposed therefore that the caves were shallow hypogenic in origin, being formed in the laterally flowing aquifer recharged from the surface in which the solutional capacity of the groundwater was enhanced by oxidation of pyrite, supposedly concentrated in specific stratigraphic rock units. This suggested origin conforms to the "geochemical" definition of hypogenic caves (i.e. caves formed by water in which the aggressiveness has been produced at depth beneath the surface, independent of surface or soil CO_2 or other near- surface acid sources; Palmer, 2000). However, it does not conform to the "hydrogeological" understanding of hypogenic speleogenesis, i.e. the formation of solution-enlarged permeability structures by water that recharges the cavernous zone from below, driven by hydrostatic pressure or other sources of energy, independent of direct recharge from the overlying or immediately adjacent surface (Klimchouk, 2014).

4 Approaches and methods

To decipher the origin of the caves, this study employed a multidisciplinary approach which included detailed speleomorphogenetic observations/surveys, studies of lithostratigraphy, geological structure (fracturing and folding) and the stable isotope composition of the host rocks.

4.1 Speleomorphogenetic analysis

A solutional cave is a macroscopic void in a rock created and shaped by moving aggressive fluids, and morphology is the fundamental attribute of the cave that reflects its origin and evolution. Thus, morphogenetic analysis of the caves aimed to reconstruct the geological controls of the speleogenesis and parameters of speleogenetic agents (fluids).

Important attributes of fluids that determine various aspects of cave morphology are their aggregate states and various modes of their movement and aggressiveness (Lauritzen and Lundberg, 2000). These attributes differ between various hydrodynamic zones, types of flow systems and components of the latter. The relationships between morphologic features (also termed forms, speleomorphs and speleogens) and speleogenetic agents have been established, although not always unequivocally, from generalizations based on field observations as well as on physical and numerical models (e.g. Bögli, 1980; Ford and Williams, 1989, 2007; Klimchouk et al., 2000; Lauritzen and Lundberg, 2000; Palmer, 2007). Although some additional ambiguity may arise from overprinting due to the sequential operation of different agents during the cave evolution, and from isomorphism, it

can be reduced or eliminated by using cross-correlated evidence and calibration of inferred agents and conditions using other methods (dating, geochemistry, etc.).

Hypogene caves are characterized by expressed morphological singularities (Klimchouk, 2007, 2009; Palmer, 2007; Audra et al., 2009a) but some forms typical for them are also common for epigene caves. Specific and diagnostic for hypogene caves is that characteristic morphs regularly occur in spatially and functionally related groups where ascending fluid-flow currents, including buoyant convection flow components, can be recognized from solutional sculptures and traced from rising inlet conduits (feeders), through transitional wall and ceiling features (rising wall channels and ceiling channels), to spherical ceiling pockets (cupolas) and outlet features (domepits). This regular combination has been distinguished as the morphologic suite of rising flow (MSRF; Klimchouk, 2007, 2009). Characteristic arrangement of individual features in MSRF and specific morpho-functional terminology is presented in Fig. 4.
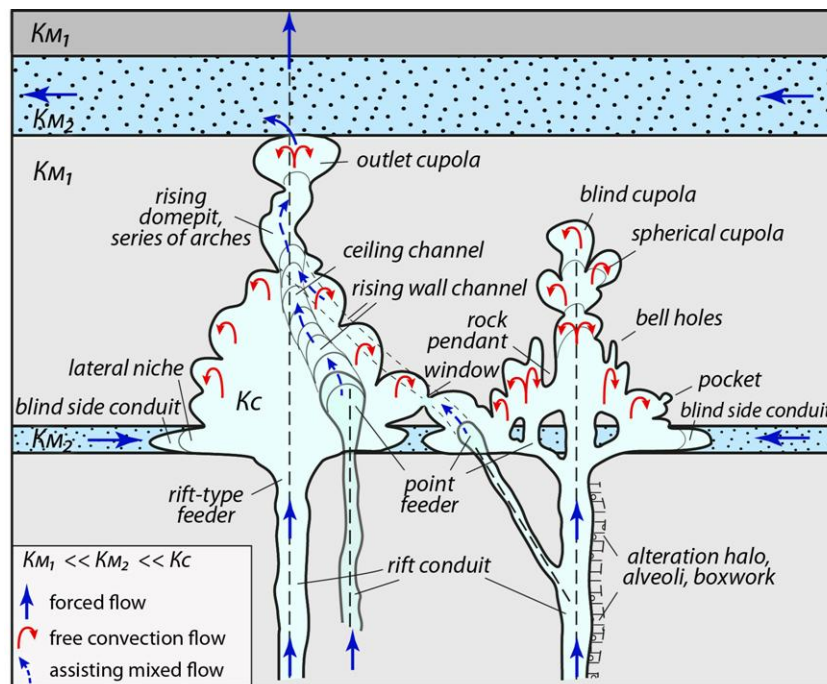
Figure 4. Conceptual representation of the morphologic suite of rising flow (MSRF), diagnostic of upwelling transverse cave-forming flow and hypogene speleogenesis (from Klimchouk, 2013). Permeabilities of different media: Km – matrix (Km1 – poorly-permeable, Km2 – well-permeable), Kc – conduits. Dashed lines indicate fractures that guided conduit development.

Morphogenetic analysis of TBV-TBR caves included: the analysis of cave macro-morphology (structure, patterns) in plan and profile, identification and classification of genetically homogenous surfaces and meso-forms, examination of spatial and temporal relationships between various

speleomorphs, and reconstruction of attributes of the cave-forming fluid system and functional roles of particular speleomorphs within the latter. The meso-morphology features of TBV and TBR, their functional relationships and relationships with geological heterogeneities were mapped in four representative key areas (Fig. 3) and systematically documented throughout the cave-wide observations. Cave patterns in the vertical and plan views have been analyzed with respect to lithostratigraphy and distribution of fractures and folds.

4.2 Cave stratigraphy approach

Overall patterns of hypogenic cave systems are guided, besides characteristics of a groundwater flow system, by initial (pre-speleogenetic) geological heterogeneities which determine preferential permeability pathways such as faults, fractures, bedding planes, and permeable beds. Their distribution in a stratified sequence is determined largely by lithostratigraphy and geological structure. Klimchouk (2007, 2013) stressed the importance of hydrostratigraphy (structure of a rock sequence from the perspective of the groundwater flow) in controlling patterns of hypogenic caves, and demonstrated that hydrostratigraphy and cave patterns can be determined not only by lithological differences but also by the vertical distribution of fractures, which does not necessarily coincide with lithostratigraphy. As speleogenesis amplifies the preferential flow pathways and reveals their pattern, the vertical distribution of voids and conduits (cave stratigraphy) is an integral expression of the hydrostratigraphy during speleogenesis.

The cave stratigraphy approach envisages subdivision of a void-conduit system into distinct storeys based on the vertical distribution of cavities. Cave stratigraphy is linked to lithostratigraphy in the following sequence: lithostratigraphy → mechanical stratigraphy → fracture stratigraphy → hydrostratigraphy → cave stratigraphy. Therefore, the cave stratigraphy approach requires coupling speleomorphogenetic analysis with detailed studies of stratigraphy, petrography and geological structure. Within this approach, components of the vertical cave pattern (storeys, connecting conduits, etc.) are identified and related to geological (sedimentary and tectonic) heterogeneities that controlled the cave-forming flow in a given flow system.

We used a detailed lithostratigraphic separation of the part of the formation exposed in the caves, based on sedimentary facies description and petrographic and petrophysical studies of the most representative layers, as described in Cazarin et al. (submitted). We have traced throughout the caves the position of voids and conduits relative to the marker units and contacts to reveal the vertical organization of the system and distinguish cave-stratigraphic storeys. The cave stratigraphy features have been related to characteristics of fractures in the stratified sequence.

4.3 Isotope studies

Investigations of stable isotope composition (carbon and oxygen) of host rocks served a dual purpose. Isotopic properties of rocks were used as an aid in stratigraphic correlation of the cave-hosting strata with more general schemes. In addition, stable isotope profiles were made in the cave walls to look for possible traces of fluid-rock interaction around fluid pathways (cave passages and bedding planes), following the approach presented in Dublyansky et al. (2014). To this end, four small-diameter (2.5 cm) rock cores up to 50 cm in length were extracted from the conduit walls, and analytical samples were taken along them at increments ranging from 1 to 3 mm. Thirty two hand specimens were taken from the quarry near Laje dos Negros village, where alteration halo of beige color has been observed around fissures. The samples representing unaltered and variously altered rocks were analyzed at random points and across the visible halo in order to look for possible associated isotope alteration.

Stable isotope analyses were performed at Innsbruck University on a DeltaPlusXL isotopic ratio mass spectrometer (Thermo Scientific) equipped with a continuous-flow preparation device (Gasbench II) following procedures described in Spötl and Vennemann (2003).

4.4 Speleogenetic analysis

Coupling the morphogenetic analysis of cave patterns and meso-forms with the study of geological heterogeneities (litho- and fracture-stratigraphy and folding) allows us to determine the mode, controls and patterns of cave-forming fluid flow, as well as the functional organization of the cave system. The notion of the functional organization of a cave system implies characterization of its components at macro- and meso-scales and relationships between them from the perspective of hydrogeological functions (recharge/throughflow/discharge) that the components have played in the cave-forming flow system. It therefore includes principal characteristics of the flow system. The functional organization of caves is a core part of a speleogenetic model. Based on morphogenetic studies and studies of cave sediments and speleothems, speleogenetic analysis also establishes phases of speleogenesis with distinct states of fluid movement and chemistry and modes of speleogenesis. Analysis of regional geodynamic history enables us to constrain the likely timing of the major speleogenetic phases, during which identified hydrogeological states and respective modes of speleogenesis could have taken place.

5 Results

5.1 Lithostratigraphy

Within the section of the Salitre Formation exposed in the caves and in the area, seven lithostratigraphic units have been identified (Fig. 5). A brief description of the units is given below,

based on a petrographic study (units 1-5) presented in detail elsewhere (Cazarin et al., submitted), with some updates from the most recent field trip (units 6-7).
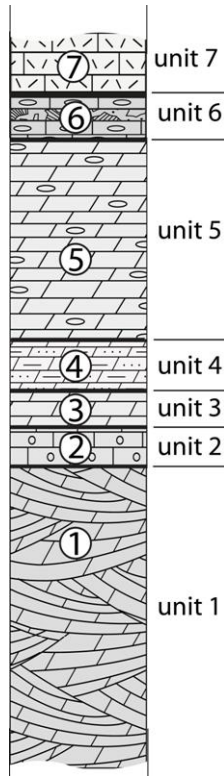

Figure 5. Lithostratigraphic section of the part of the Salitre Formation exposed in the TBV and TBR caves (modified from Cazarin et al., submitted). See text for description of units.

Unit 1 is the lowermost part of the succession exposed in the caves. It is comprised of massive oolitic grainstone with cross-bedding planes. The maximum thickness of this unit could not be established because the accessible cave system does not reach its bottom, but the visible thickness is 12-15 m.

Unit 2 is fine oolitic, peloidal grainstone with intraclasts. The beds are 0.5-1.0 m thick and exhibit plan-parallel stratification and concentric chert nodules sized at 10-30 cm. The unit has the thickness of 1.5-2.0 m. Zoned dolomite rhombohedrons are identified in thin sections from these rocks (Cazarin et al., submitted) that may indicate interactions of the rocks with hot brines (Spötl and Pitman, 1998).

Unit 3, up to 1 m in thickness, consists of microbial carbonates with laminites, columnar stromatolites and thrombolites. Examination of thin sections provides evidence of hydrothermal activity such as silica-infilling of vugs and fractures (Cazarin et al., submitted). Whether such alteration was related to the speleogenesis or was areally pervasive is not clear.

Unit 4 is comprised of a densely stratified, predominantly siliciclastic, succession of siltstones, fine-grained sandstones, clays and marls, 1.5-2 m in thickness. Layers of peloidal grainstone with chert nodules a few cm thick also occur in this unit. The contacts with the adjacent units are distinct. Unit 4 pinches out in some areas of TBV (Sector C in Fig. 3) and, likely, is absent through the most of the TBR area. Since this unit is readily recognizable in the cave walls, it was used as a main marker to establish the stratigraphic distribution of cavities.

Unit 5 is comprised of densely to moderately bedded grainstone intercalated with numerous 1-10 cm-thick chert layers. The thickness of the unit is up to 10-12 m.

Unit 6 is composed of 10-30 cm-thick carbonate layers of pink color intercalated with discontinuous 1-3 cm-thick layers of dark shales. The thickness of this unit is about 1.5 m. A more continuous shale layer ca. 10 cm in thickness separates this unit from the overlying Unit 7. Embedded

12

within Unit 6 are fragments, 3-15 cm in size, of a light grey carbonate rock, which exhibit stratiform distribution. This breccia-like layer of grey color ca. 20-30 cm in thickness occurs in the lower half of the unit. As most of the caves lay below Unit 5, Unit 6 is accessible only in Sector D (Fig. 3) of TBV.

Unit 7 is composed of laminated carbonate mudstones, with chert lenses and numerous cm-sized vugs lined with small calcite crystals. The lower part of the unit is observable only in collapsed areas of sector D of TBV and represents the stratigraphically highest level accessible in the TBV-TBR system. The unit continues upward to the surface, which lies 15-20 m above this cave area. A further 15-20 m higher stratigraphically, fresh exposures of the Salitre Formation are observed in quarry faces NE of the Laje dos Negros village (see Fig. 2). We consider the quarry section to be an upper part of Unit 7. Fresh rock surfaces in the quarry display distinct alteration halos of beige color, extending symmetrically for 1-10 cm on both sides of certain bedding planes, bedding-parallel stylolite seams, and joints (Fig. 6). We observed such an alteration halo also around a solution cavity 15-20 cm in size, developed along a vertical joint (Fig. 6D). Meanwhile, the halo is not observed around of large rift-like passages exposed in some quarry faces.

Figure 6. Alteration halos along bedding planes, stylolite seams and joints in the Salitre dolomites: A - in the Toca da Boa Vista, B-D – in a quarry near the Lage dos Negros village.

In some areas of TBR we identified meter-scale bodies of breccia within Unit 1, mainly irregular in shape. The breccia consists of angular clasts of the host rock of sub-meter size floating in dense dark-grey micritic cement, well lithified and devoid of allochtonous material. These bodies are intersected by the dissolution surfaces of the main cavities, indicating that the breccia was already in place by the time of the main speleogenetic phase (Fig. 7).

Figure 7. Breccia body in Unit 1, Toca da Barriguda.

Some narrow vertical breccia bodies, apparently unrelated to the breccia described above, are aligned along major faults and fractures, intersecting units 1-4. In this fault breccia, we observed (in thin section) minerals related to thermal, possibly H_2S-bearing fluids, such as saddle dolomite, quartz, barite, gypsum, and pyrite.

All the Salitre Formation rocks exposed in the area are indurated, well lithified, and have low matrix porosity, commonly within the range of <1 to 7 % (Cazarin et al., submitted). The pre-speleogenetic permeability of these rocks was strongly dominated by joints, faults and bedding planes, which guided the development of conduits.

5.2 Folding and fracturing

Besides lithostratigraphy, folds and fractures are important geological heterogeneities that could control fluid flow and conduit development in these caves. Results of detailed studies of the folding and fracturing will be presented elsewhere; these structural features are briefly summarized below in order to set a stage for speleomorphogenetic analysis.

14

The Salitre Formation in the area is characterized by gentle folding (Fig. 8A), which is probably a far-field response to the intense deformation that took place along the encircling Brasiliano thrust and fold belts (Brito Neves et al., 2014). Folds observable in the caves are non-cylindrical and linear over distances of tens to hundreds of meters, forming a system of sub-parallel anticlines and troughs with N-S dominant orientations, but ENE-WSW and NW-SE-trending fold axes are also present. The distances between crests of adjacent anticlines vary between 60 and 120 m; amplitudes of undulation are commonly within 3 to 10 m. A deeper structural depression is found in Sector D (up to 20 m relative to adjacent sector C). Folding is best observed in the caves in the well-bedded stratigraphic units, 3-4.
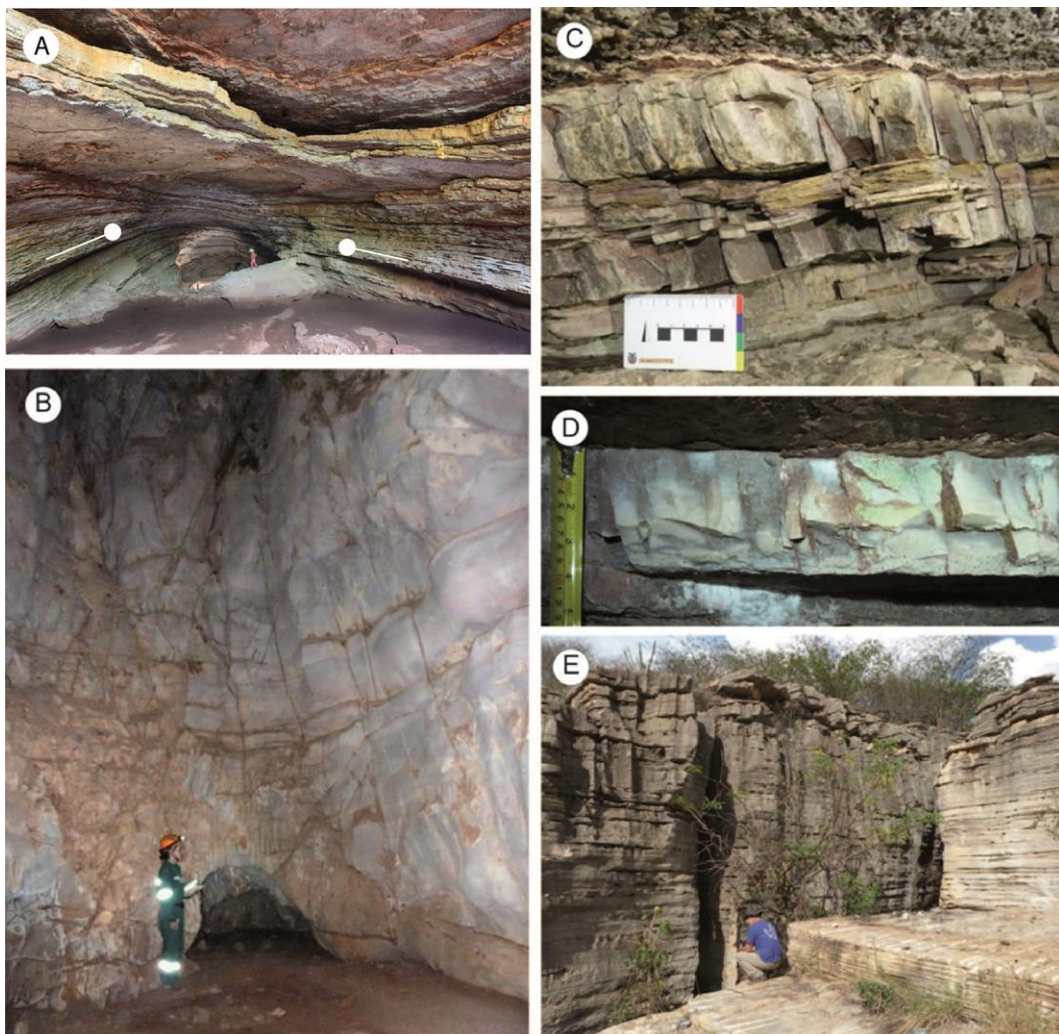

Figure 8. Folds and fractures in TBV: A – large NEE-SWW-trending fold that controls the entrance passage of the cave; B – large fractures in Unit 1; C – stratabound joints in Unit 4; D – tectonic stylolites in Unit 4; E – large sub-vertical fractures in Unit 7 (in the quarry).

Fractures in the Salitre Formation mostly consist of veins, joints, and tectonic stylolites (Fig. 8). Veins and joints in the lower massive grainstone of Unit 1 are spaced ca. 1-3 m, and their vertical length (height) is generally several meters and more, often greater than visible bed thickness (Fig. 8B). The spacing between adjacent joints and veins in the well-bedded units 3-4 ranges from few mm up to 10-15 cm; most of veins and joints there are strata-bound (Fig. 7C). Tectonic stylolites are best developed in clay-dominated siltstones of Unit 4 (Fig. 8D). They are sub-vertical, orthogonal to bedding, spaced 5-15 cm, and consistently strata-bound. The fracture pattern in Unit 6 is similar to Unit 4, i.e. closely spaced and strata-bound fracture systems. The upper laminated dolomite of Unit 7 is characterized by extensional fractures spaced 3-6 m and 4-8 m in height (Fig. 8E).

In Unit 1, besides smaller background fractures of moderate to low frequency, of particular importance for speleogenesis are large, sub-vertical or steeply inclined, fractures that have traceable vertical extent of up to 10-12 m. Most of them terminate upward within Unit 2 or a few meters below it. The large fractures in Unit 1 occur in swarms, in which spaces between fractures in a set vary from 1-2 m to 5-8 m. These fracture swarms control clusters of cavities occurring in the lowermost storey of the cave. Only few fractures in fracture swarms penetrate upward far enough to reach units 3-4.

Unit 2 does not differ significantly in overall density of small background fractures from Unit 1, but units 3 and 4 are much more densely fractured, with spacing ranging between few mm to few dm. Unit 4 has the greatest stratification and fracture density, favoring lateral flow and conduit development in this stratigraphic level.

Unit 5 generally has a very low density of fractures, notably in its lowermost part, which acts as an aquitard (a "seal" in reservoir terminology). However, there are isolated large vertical fractures, or broadly spaced (4-8 m) clusters of such fractures, which start in units 3-4 or in even lower units and penetrate upward for many meters across units 5-7. Such fractures control passages of characteristic rift-like morphology that hold the uppermost stratigraphic position in TBV and occur in the quarry and the cliff near the Laje dos Negros village.

5.3 Cave morphology

The patterns of caves represent their macro-morphology, i.e. the arrangement of the various components that form a system. Patterns are determined by hydrodynamic factors, geological heterogeneities that favor or impede fluid flow, and the geomorphic evolution or the area. The components of patterns are conduits (passages of various shapes and sizes) and voids (chambers, rooms, etc.), whose shapes and major features of the internal relief characterize the cave meso-morphology.

5.3.1 Macro-morphology: cave patterns in the vertical and plan views

Following the cave-stratigraphic approach outlined in Section 3, we used the lithostratigraphic division (Section 5.1) to trace throughout the area the vertical position of different components of the cave system within the sequence. Unit 4 and its contact with Unit 5 were used as markers. Three cave-stratigraphic storeys have been distinguished, although they are not hypsometrically invariable because of folding (Figs. 9, 10). These storeys differ considerably in patterns and morphology (Fig. 11).
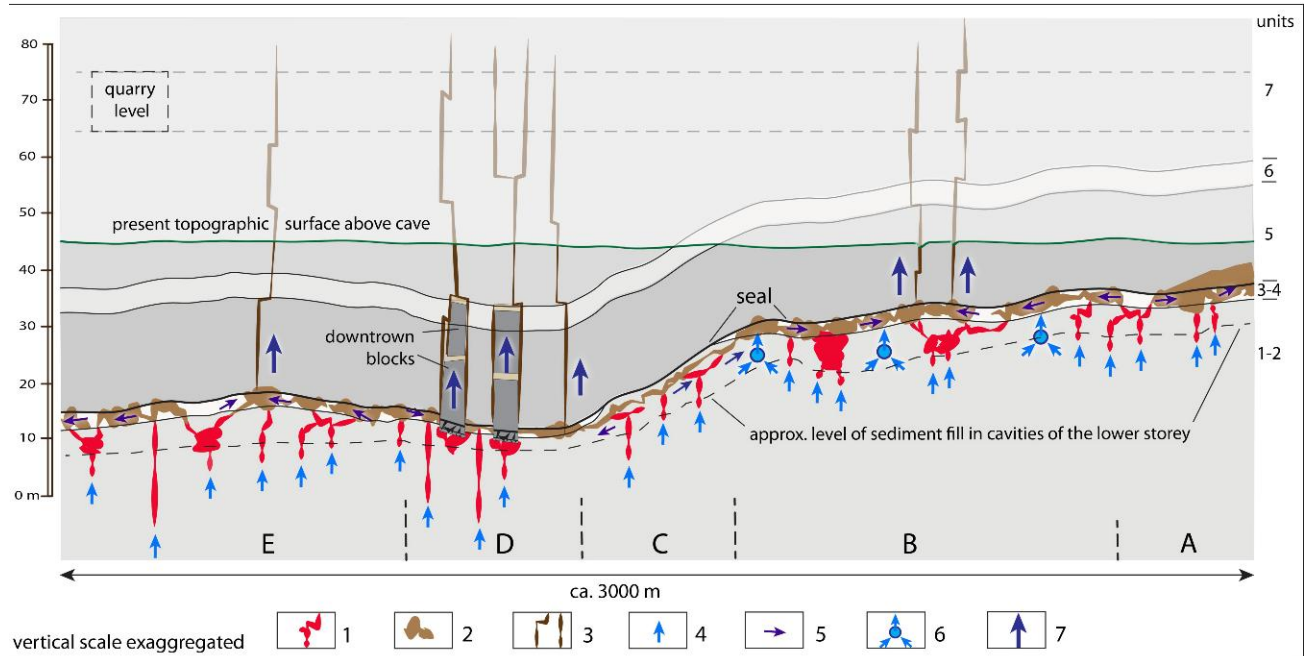

Figure 9. Vertical structure and functional organization of TBV, shown along the NE-SW-oriented schematic composite profile. A-E - sectors of the cave (cf. Fig. 3). 1 - 3 - cavities in different storeys: 1 - lower storey (recharge components), 2 - middle (master) storey (lateral distribution components), 3 - upper storey (outflow components), 4 - 7 - inferred directions and components of flow: 4 - inflow from below, 5 - lateral flow, 6 - lateral drainage to master passages from tributary sub-systems (cf. Fig. 16 upper left inset), 7 - outflow toward discharge boundary above.

The lower cave-stratigraphic storey is comprised of cavities developed mainly within lithostratigraphic Unit 1, i.e. the massive oolitic grainstone. These cavities are represented by clusters of passages controlled by large vertical fractures, chambers of different sizes, and isolated conduits (Fig. 11G-I). The passage clusters consist of series of parallel passages or small rectilinear networks, oriented NE-SW and NW-SE and terminating abruptly in lateral directions (Fig. 12A). Closely spaced passages in clusters often coalesce at some levels, which produces chamber-like morphologies with pillars and rock pendants hanging from the ceilings (Fig. 12C). The coalescence of adjacent individual

17

forms produced by rising flow into an integrated space, resulting in sculptured protrusions and the division of the cave into "highs" and "lows", was described as "integration" by Osborne (2007), based on observations in Australian hypogene caves. Heights of passages and chambers vary in short distances along profiles due to a presence of many cupolas and domepits in the ceilings (Fig. 11G). Chambers commonly have blind-terminated passages and alcoves at their sides and many high solution pockets, phreatic domepits and channels (half-tubes) in the ceilings (Fig. 11H-I), which produces ramiform patterns. Some chambers in this storey are very large in plan view, especially those along the north-eastern and southern edges of TBR.
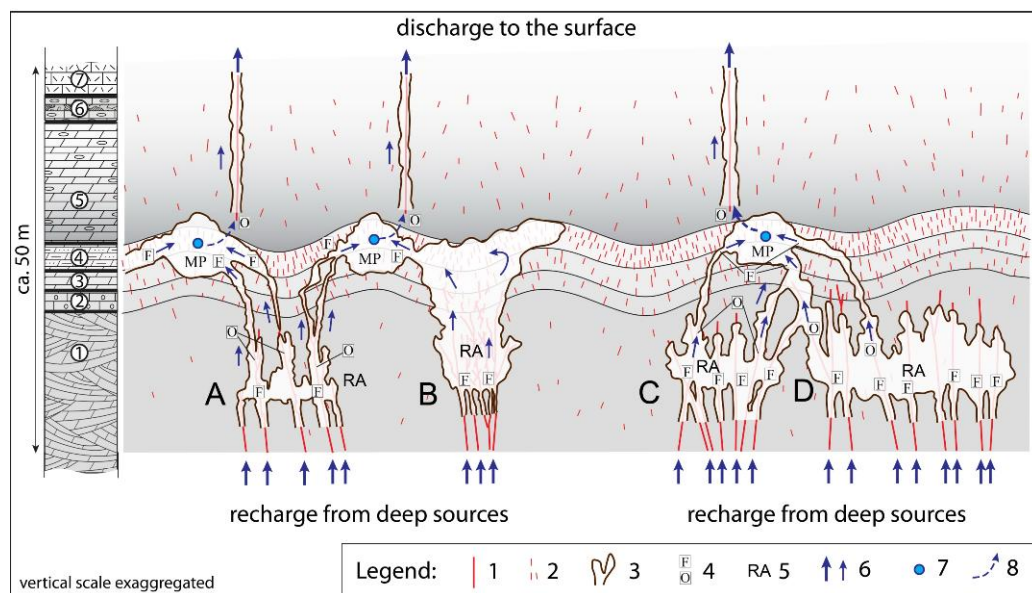

Figure 10. Details of the vertical structure and functional organization of the cave system (conceptual model). Lithostratigraphic units (column in the left) as in Fig. 5. 1 - major fractures intersecting the bed contacts; 2 - minor fractures (predominantly strata-bound joints); 3 - solution cavities; 4 - functional elements of caves: at meso-scale: F - feeders, O – outlets; at macro-scale: MP – master passages, RA recharge areas; 6 - flow directions; 7 - lateral flow in the direction normal to the profile plane; 8 - convergence of lateral flow to outlet conduits in the upper unit.

Chambers and passage clusters of the lower storey connect to passages of the overlying middle storey via some of the highest domepits or rift-like conduits (clusters A, C and D in Fig. 10; Fig. 12B), but sometimes they connect via large inclined passages or directly merge upward with the middle storey, creating large and high chambers (cluster B in Fig. 10; photo F in Fig. 11). In TBV, clusters of lower-storey cavities are commonly isolated from each other at their own level in any lateral direction, even when cavities of adjacent clusters come close to each other (Fig. 12A). This strongly suggests that there was no cave-wide lateral through-flow in this storey.

Figure 11. Morphotypes of cavities occurring at different cave-stratigraphic storeys. A through D – rift-type passages in the upper storey: A and B – in the cliff in the south-eastern edge of the Laje dos Negros village (Unit 7), C – in the quarry on the north-western edge of the village (Unit 7), D – in sector D of TBV (Unit 5). E and F – master passages in the middle storey (units 3-4): E – common morphology, F – merging of cavities of the lower and middle storeys (a view from the middle storey passage). H through J – cavities in the lower storey (Unit 1): H – a fracture-controlled passage, I and J – large chambers.
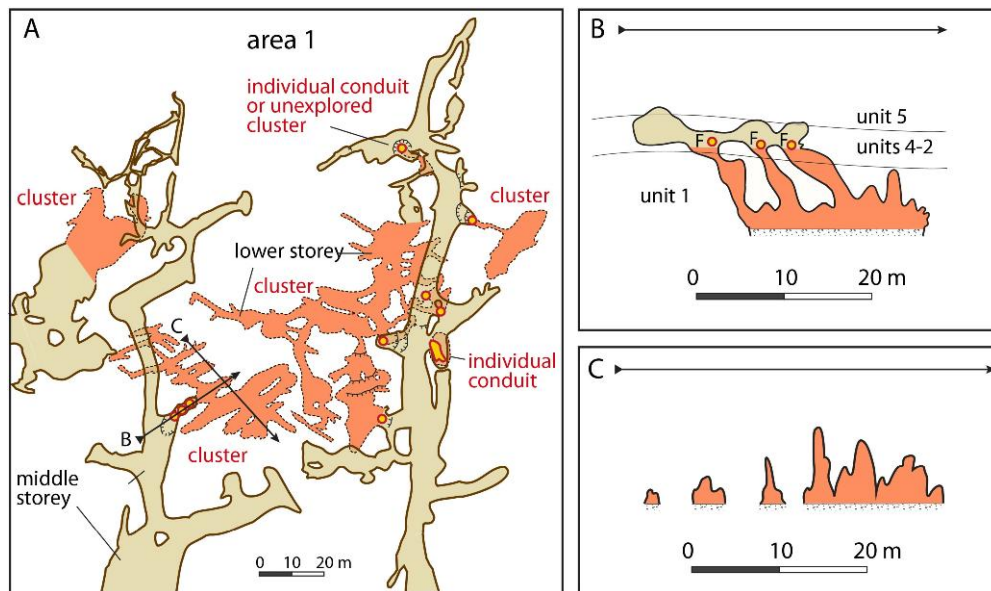
Figure 12. Stratigraphic differentiation of cavities in TBV and cave patterns at the lower and middle storeys within area 1 in TBV (for site location see Fig. 3). Circles indicate feeders as seen from the middle storey, corresponding to outlets in the lower storey (see section 5.3.2 for explanation of these features).

The middle cave stratigraphic storey is comprised of passages developed within lithostratigraphic units 3 and 4. It is present almost everywhere throughout TBV (except parts of Sector C) but in TBR occurs only in the NE part. Its largest and longest passages ("master passages") are developed sub-horizontally, generally along the crests of anticlines (Fig. 10) trending mainly N-S and NNE-SSW, although ENE-WSW oriented passages with the same control are also present. Master passages commonly have a near-rectangular shape in cross-section (Fig. 11E), width 4-12 m and height 2-6 m. Individual passages of the N-S set can stretch for many hundreds of meters (up to 700 m in Sector E in the south-west of TBV). Smaller, inclined passages in this storey are oriented perpendicularly or diagonally to master passages, originate within structural troughs at points of connection with the lower storey and join master passages from their sides. Sometimes they connect adjacent master passages across dividing troughs. The ceilings of passages in the middle storey are controlled by siltstone layers of Unit 4 or by the base of Unit 5 (Fig. 11E), extending above the latter for not more than 1-2 m in some larger ceiling pockets and channels (Fig. 11F) or in areas of slab breakdown.

The upper cave-stratigraphic storey is represented almost exclusively by rift passages developed along large sub-vertical W-E-trending fractures that pass through lithostratigraphic units 5 and 6 and

extend up into the overlying unit 7 (Fig. 11A-D). Rifts in Unit 7 commonly have roughly parallel walls and uniform widths at certain altitude intervals (Fig. 11A-C), but in Unit 5 many chert beds protrude into the passages making the vertical wall profiles jagged (Fig. 11D). Chert layers often form horizontal partitions that almost completely close the rift, broken only by the original fracture. In places, rifts remain narrow through the most of their length, but there are wider (up to 2-3 m) vertical conduits with oval cross-sections aligned up the central fracture. Such are the two shaft-like entrances in TBV that connect the cave to the surface in Sector B. In Sector D (Fig. 3) the mapped cavities are chiefly these rift passages in Unit 5, plus breakdown chambers formed by downward displacement of blocks between adjacent rifts. Passages of this rift-type morphology are also observed in the quarry and in the cliff at the outskirts of the Laje dos Negros village (Fig. 11A-C), i.e. in the upper part of the lithostratigraphic Unit 7. Based on this observation, we propose that combinations of rift-type conduits of the upper storey originally extended for many tens of meters above the middle storey, as shown in Fig. 9, but that a large part of this storey has been eroded away.

The overall plan pattern in TBV is determined by the superposition of cavities mainly in the lower and middle storeys and is largely a reticular maze. In Sector C, however, the pattern is peculiar due to specific structural and lithostratigraphic conditions (Fig. 9). Here, on a structural slope, lithostratigraphic Unit 4 is absent and passages in the middle storey develop within the upper part of Unit 1 and in units 2-3. They are smaller than common passages in this storey, have variable sculptured morphology and form more densely packed network. The lower storey in this sector is represented mainly by individual sub-vertical and inclined conduits. Also peculiar is the cave pattern in Sector D, where mapped cavities are chiefly rift passages and breakdown chambers of predominantly W-E orientation. In TBR, the plan pattern is comprised by chambers and passages in the lower storey throughout most of the cave and is a combination of rectilinear and ramiform components. This cave is dominated by large ramiform chambers except parts along the SE edge, where there is a rectilinear pattern of fracture-controlled conduits.

Cave-wide lateral connections in TBV occur mainly via the middle storey passages. Only in few places in the cave are adjacent regions of the middle storey connected laterally via passages of the lower storey. In Sector D, physical lateral connection is provided by rifts and breakdown chambers in the upper storey. In TBR, conduits and voids of the lower storey are laterally integrated into one huge cluster, within which several sub-clusters can be distinguished, laterally connected by single passages alone.

5.3.2 Meso-morphology

Meso-morphology features have been surveyed in detail in four key areas and systematically documented during numerous cave-wide traverses. The most important generalizations are as follows: (a) the caves completely lack speleogens related to vadose streams and downward circulation; (b) phreatic speleomorphs indicating rising flow are widespread, being arranged in spatially and functionally related assemblages that classify as "morphological suites of rising flow" (see section 4.1 and Fig. 4), which are diagnostic for hypogenic speleogenesis (Klimchouk, 2007, 2009; 2013); and (c) the distribution and appearance of meso-forms is distinct in the different storeys.

In MSRF, the most important features, in terms of functionality, are feeders - vertical or inclined conduits that connect to a given cavity from below and supplied rising flow to it during the main phase of speleogenesis. There are several morphological types of feeders in the TBV-TBR system (Fig. 13). Rift-type feeders are solutionally enlarged sub-vertical fractures (Fig. 13A-C). Some prominent rift-type feeders are up to 10 m deep, reaching the modern water table or clogged at the bottom with sediments. Funnel-type feeders are point features with funnel-shaped orifices (Fig. 13D-F). Side feeders occur in the lower parts of the walls (Fig. 13E, G-I) and commonly have inclined (rather than vertical) conduits controlled by bedding.

Feeders in the bottom of cavities of the lower storey supplied rising fluids to the cave system. As they are buried or clogged at shallow depth by sediments, their actual depth is unknown. Locations of buried feeders are indicated by funnel-shaped hollows in sediments, by alcoves and rising channels in the walls (Fig. 14J) and by cupolas in the ceilings (Fig. 15B). Large individual clusters of lower storey cavities have many tens of the feeders in the bottom.

Some feeders in passages of the middle storey (units 3-4) have sub-vertical conduits coming directly from the lower storey cavities, but most of them are side feeders with inclined bedding-controlled conduits (Fig. 13G, H). Side feeders are especially common in passages that follow the crests of anticlines, occurring on both sides of them (Fig. 16 upper left inset). Although feeders often occur in localized clusters, at the scale of the whole cave they are scattered more or less uniformly along the middle storey passages.

Side feeders commonly occur below alcoves and/or rising wall channels. The latter may lead immediately into a cupola or continue in the ceilings to end up at a more distant cupola or domepit (Fig. 14). Domepits represent outlet features which convey rising flow to the upper storey.

Figure 13. Feeders in the TBV-TBR system. A through C – rift-type feeders, D through F – funnel-type feeders, G through I – side feeders.

Figure 14. Rising wall- and ceiling channels, cupolas and domepits (outlets). A-C – outlets in the middle storey cavities (looking up from below), D-J – various features in the lower storey cavities. All photos but D, F, G and J are views up from below. D – domepit (outlet); E – ceiling channel and cupolas; F - wall and ceiling features associated with a side feeder; H – rising chain of cupolas arranged in a channel, ending at the domepit (outlet); I – chains of cupolas: left – ending at the outlet, right – blind; J – alcove and rising wall channel above inferred feeder in the passage dead-end, and the outlet in the ceiling.
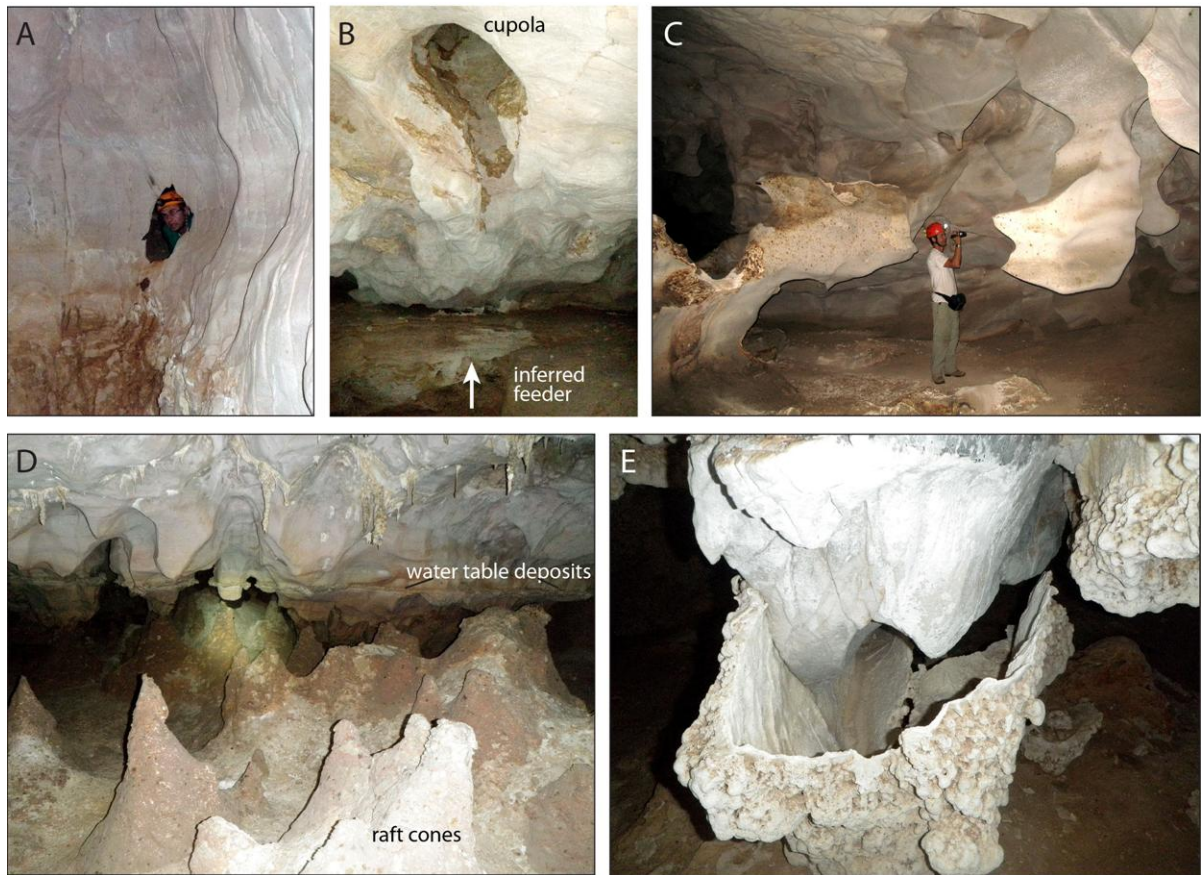
Figure 15. Some specific features of cave morphology in the lower storey of the cave: A – a window in a thin wall partition, separating adjacent chambers in the lower storey, B – an example of feeder-cupola matching relationship, C – large rock pendants possibly additionally sculptured by subaerial weathering, D – morphological and speleothemic indications of the water table conditions, E – subaerial weathering of dolomite on a pendant beneath the calcite crust.

The wall and ceiling sculpturing by rising flows is especially prominent in cavities of the lower storey (Fig. 11H, I; Fig. 14D-J). This is due to the following reasons: (1) the proximity and high density of original feeders that supplied upwelling aggressive water to the cave, (2) the important role of natural convection and upward-propagating buoyancy dissolution, and (3) the massive bedding in the Unit 1. In large chambers in the lower storey of TBR there are hundreds of closely spaced blind cupolas, overlying depressions in the bottom. Some cupolas often assume the shape of "bell holes" – blind vertical tubes of constant diameter in which height is much greater than width. Such features are interpreted as indicators of very stable convection circulation cells (Birmingham et al., 2011).

Wall and ceiling features are less well expressed in master passages of the middle storey because of: (1) the thin bedding of the host rock in Unit 4 and common presence of siltstone and chert beds in contact with Unit 5, (2) slab breakdown processes that partly destroyed original solutional

sculpturing, and (3) the presence of lateral flow components that prevent establishment of sustained convection cells. Homogenization of fluid temperatures and dissolved solids contents along flowpaths from lower storey feeders to middle storey master passages probably also reduced the potential to form local distinct buoyant dissolution features. Wide and smooth cupolas and ceiling channels are characteristic of places where large lower-storey cavities directly merge with the master passages (Fig. 11F); alternatively, they occur above feeders that connect large lower storey clusters to the master passages.

The outlet features from the middle storey are much less frequent than in the lower storey. They are vertical rift-like conduits (Fig. 14A) or oval in plan shaft-like conduits aligned in large fractures (Fig. 14B, C) that breach the integrity of the seal in the lower part of Unit 5. Sector D is the locus of rift-like outlets in TBV, and several isolated outlets are known in sectors E and B. Two outlets in the middle of Sector B (Fig. 16) are vertical shaft-like entrances to the cave (Fig. 14C). Such features are not known in TBR.

Other common features of meso-morphology, mainly occurring in the lower storey, are partitions between adjacent passages or chambers. They often have sharp-edged windows suggesting the virtual absence of lateral flow (Fig. 15A). Also common are rock pendants (Fig. 15C). These features illustrate lateral coalescence of cavities and indicate rising flow patterns and/or convective circulation (Klimchouk, 2007, 2009).

There are indications of water-table conditions in many chambers and passages of the lower storey (Auler and Smart, 2001): calcite shelfstones (rims) traceable at the same level across a cave cluster, raft accumulations and cave cones, subaqueous coatings and coralloids. Rock pendants and partitions show no thinning below the water table (Fig. 15D) and there is no horizontal notching in the walls associated with the water table, which suggest that the water was not aggressive during the water-table phases. However, there are clear signs of wide-spread subaerial dissolution and weathering above the former water table, which have affected many of the surfaces, especially in proximity to the outlets connecting cavities at the lower and middle storeys. Subaerial dissolution due to condensation corrosion above thermal lakes is known to be a potent mechanism for modification of cave meso-morphology (e.g., Dublyansky and Spötl, 2015). In the TBV-TBR system, subaerial dissolution of micrite in the host dolostones promoted arenitization and formation of dolomitic sand ('grus') below surfaces affected by condensation corrosion (Auler, 1999). Based on observations of the dissolved subaerial speleothems and rock pendants (Fig. 15 E) and the accumulations of grus, subaerial weathering could have consumed up to several tens of centimeters of the rock (Auler and Smart, 2004).
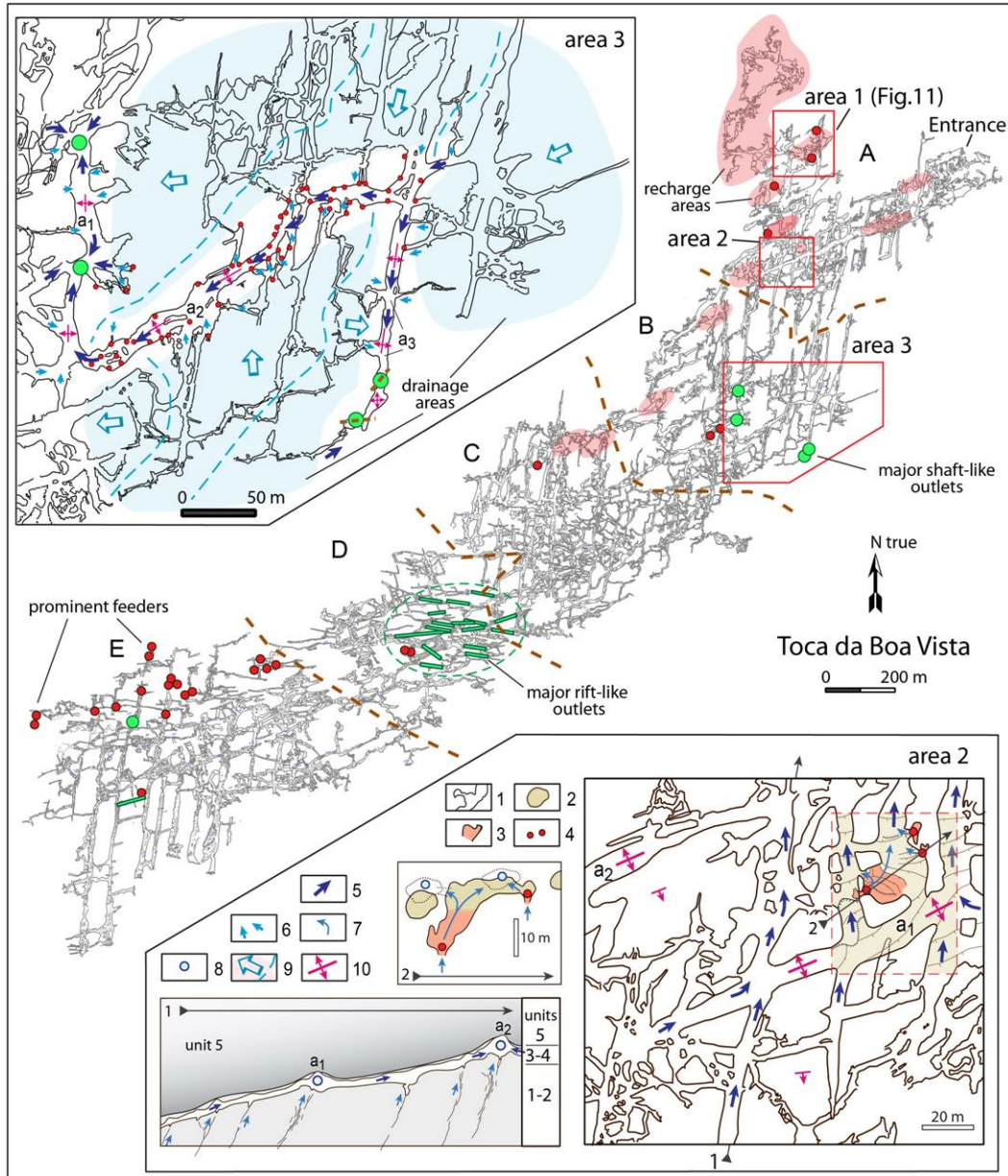
Figure 16. Distribution of major recharge and discharge features across TBV and details of the cave morphology within selected areas (insets) showing functional organization of the cave in the plan view. Passage network is mainly in the middle storey, functioning to laterally distribute flow from prominent feeders and recharge areas to the outlet features. Insets in the upper left and lower right show details of the functional organization within the key areas 2 and 3, as reconstructed from morphogenetic mapping (see text for discussion). Legend for insets: 1 - cave passages (mainly in the middle storey); 2 and 3 (for area 2) - cavities in the middle and lower storeys, respectively; 4 - individual small feeders (in the area 3 mapped only in the a2 passage; not mapped in the area 2, where only three major feeders are shown by circles); 5 - directions of concentrated flow; 6 (for area 3) - directions of tributary inflows to major flow paths from subordinated passage systems; 7 (for area 2) - individual inflows from feeders; 8 (for area 2 profiles) - lateral flow in the direction normal to the profile plane; 9 – (for area 3) approximate boundaries of drainage areas and general directions of lateral drainage in individual drainage areas; 10 - hinges of anticlines. a1 - a3 - master conduits developed along the hinges of anticlines.

5.4 Isotopic analysis of the karstified rocks

Oxygen and carbon isotope ratios have been determined in dolomites of the Salitre Formation, freshwater Caatinga limestone and samples of secondary calcite collected from voids in the Caatinga limestone. The results plus some data for these rocks from the literature are shown in Fig. 17.
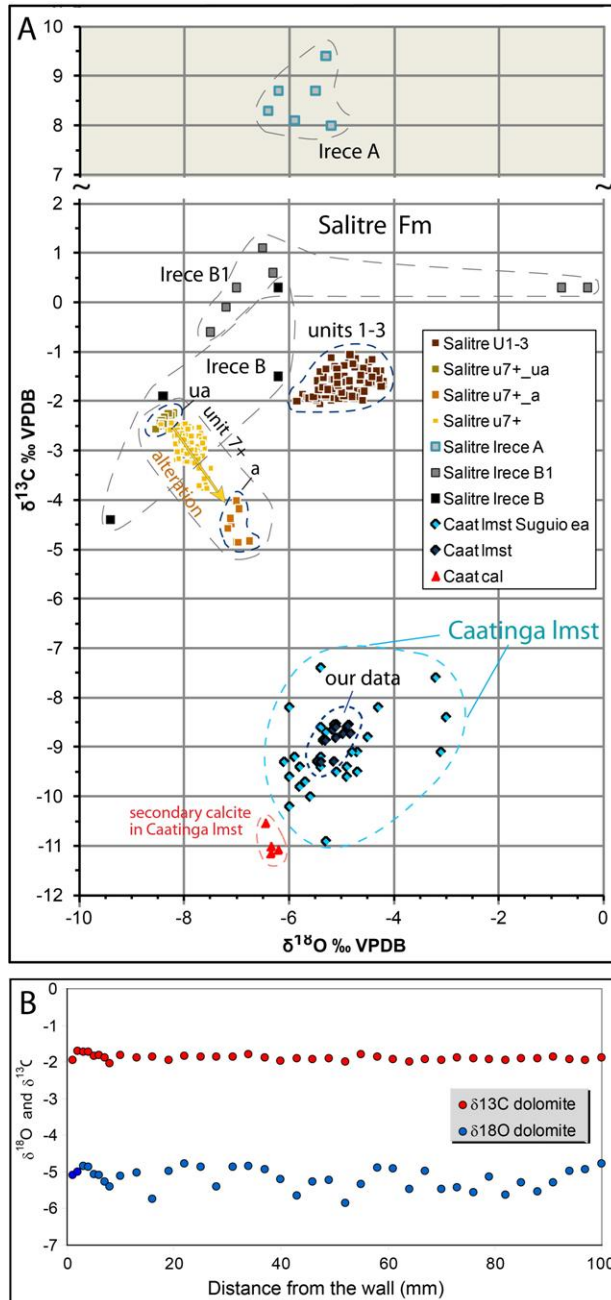

Figure 17. A - Oxygen and carbon isotope properties of the Salitre and Caatinga carbonates from the Campo Formoso area. Alteration trend for Unit 7 dolomites is indicated by an arrow. Irece A, B and B1 indicate values from units A, B and B1 of the Irecê Basin (data from Misi and Kyle, 1994; Misi and Veizer, 1998; Misi et al., 2007). Data from Sugulo et al. (1980) for the Caatinga limestones are included. B - Oxygen and carbon isotope profiles along the P1 core drilled in the wall of a TBV conduit in Unit 2.

Four 9-20 cm-long mini-cores were taken from the walls in TBV in units 1-3 in order to look for possible isotopic alteration around conduits attributable to fluid-rock interaction. Profiles along the cores (sampling at 1-3 mm increments) produced 112 paired C and O isotope measurements. In Fig. 17A the δ^{18}O and δ^{13}C values of units 1-3 plot within a compact field. Average δ^{18}O is -4.9±0.4 ‰ and average δ^{13}C is -1.7±0.2‰ (variations at 1σ-level). The profiles along the cores are essentially flat (Fig. 17B); no systematic variations were observed. This suggests that either there were no isotopic alteration resulted from interaction of the conduit fluids with the rock, or the altered zone was thin and completely removed by later processes (dissolution and/or subaerial weathering).

We have also analyzed samples from the quarry near Laje dos Negros village, which represent the upper part of Unit 7 (Salitre u7+ in Fig. 17A). The set of 24 samples of the unaltered (grey) rock yielded average values of $\delta^{18}O$ at -8.4±0.1 ‰ and $\delta^{13}C$ at -2.4±0.1 ‰. Relative to the average values for units 1-3, the composition of the rock in Unit 7 is slightly depleted in carbon (by 0.7 ‰) while oxygen is depleted by 3.5 ‰.

Another set of samples (n=8) from this unit was taken to represent the presumably altered rock that displayed the most intense and uniform beige coloration (see Section 5.1 and Fig. 6B-D). These samples yielded average values of $\delta^{18}O$ of -7.0±0.1 ‰ and $\delta^{13}C$ of -4.5±0.3 ‰. Relative to the unaltered rock, $\delta^{13}C$ is significantly displaced toward lower values (by 2.1 ‰), whereas oxygen is enriched in the ^{18}O isotope by 1.4 ‰. This alteration trend is shown by an arrow in Fig. 17A. $\delta^{18}O/\delta^{13}C$ points of samples with less intense coloration and those taken across the bedding and variously colored zones (n=96) scatter between these end members, demonstrating a strong negative correlation between the isotopes (r = −0.72). This linear trend, as well as the location of colored zones around bedding planes and joints (see Fig. 6B-D), suggest that color- and isotopic alterations were caused by post-diagenetic water-rock interaction. Calculations of limits suggest that the interaction occurred at relatively low temperatures: not exceeding 65°C if the reacting water had $\delta^{18}O$ = 0 ‰ SMOW (seawater) or 35°C if water had $\delta^{18}O$ = -5 ‰ SMOW (meteoric water; in these calculations we assumed that the rock became completely equilibrated with the reacting waters).

Our data for one hand specimen of the Caatinga limestone ($\delta^{18}O$ = -5.1±0.2 ‰, $\delta^{13}C$ = -8.8±0.3 ‰; n = 15) fall within the broader field reported for this limestone by Suguio et al. (1980). Secondary calcite that lines solution voids with phreatic morphology found in this limestone show that both $\delta^{18}O$ and $\delta^{13}C$ values are depleted in heavy isotopes compared to the rock, by about 1.2 ‰ and 2.1 ‰ respectively. Calculations suggest that the temperature of deposition for the secondary calcite was relatively low, not exceeding 33°C if the mineral forming water had $\delta^{18}O$ = -5 ‰ SMOW and still lower for isotopically lighter waters.

6. Discussion

6.1 The depth of burial of the cave-hosting carbonates

Correlation of the cave-hosting sequence in the Campo Formoso area with the broader stratigraphic schemes, based mainly on chemostratigraphy, suggests that it likely belongs to the lower part of the Salitre carbonate mega-sequence (Fig. A1, Appendix), which means that the cave-hosting sequence has been once buried to considerable depth. Based on the assumption that the base of the formation in the cave area lies no deeper than 200 m below the caves but the thickness of the formation

reaches 1000 m in the wider region, it can be inferred that about 800 m of overlying carbonates have been denuded. Widespread presence of bedding-parallel stylolites, which form most effectively in the depth range of 600-900 m (van Golf-Racht, 1982) suggests similar depths of burial.

It is not known if the Salitre Formation was ever covered by other Neoproterozoic or younger rocks in the Campo Formoso area. A study by Japsen et al. (2012) based on apatite fission track data demonstrated that, after the Early Cretaceous break-up which separated South America from Africa, the present land surface was buried below a 2-3 km-thick cover across the east Tucano rift and the interior highlands, up to ca. 200 km west, which encompasses the study area (Fig. 1). This cover was almost completely removed during Campanian and Eocene uplift phases, followed by Oligocene–Miocene reburial and uplift and exhumation in the later Miocene. Multiple phases of burial and denudation after Early Cretaceous have been also established in the Borborema Province, a collection of fold belts to the north of the São Francisco Craton, where the overall denudation since break-up was estimated at 1 to 3 km by Morais Neto et al. (2009) and at 3-4 km by Nóbrega et al. (2005).

This cursory analysis indicates that the cave-hosting part of the Salitre Formation, before it was brought into shallow subsurface in the post-Miocene time, experienced long and complex burial history, during which it could be repeatedly affected by deep-seated fluids.

6.2 The cave-forming flow system and geologic controls over fluid flow

This study reinforces the conclusion of Auler and Smart (2003) that the TBV-TBR cave system has been formed in phreatic conditions. In addition to the lack of vadose morphological features and sediments that would indicate free-running streams, there are no indications in the cave pattern and morphology that the caves received any recharge from the surface in the past.

The three-dimensional pattern of the cave system does not conform to the conditions of a shallow laterally-flowing aquifer, in which a systematic gradient toward a nearby erosional valley would exist. Cavities of the lower stratigraphic storey are clustered, and the clusters are scattered across the cave fields and laterally isolated from each other. Even more isolated are rare conduits of the upper stratigraphic storey. Although conduits in the middle storey do form laterally extensive networks, even there the networks are not continuous across the entire cave field, and there are no systematic changes in the cave pattern and morphology in any lateral direction as would be expected if the caves were formed by lateral flow. Locally recognizable indications of lateral flow point to flow in different directions even in adjacent parts of the network (Fig. 16 upper left inset).

In contrast, there is ample morphological evidence for ascending flow across the Salitre Formation during the main speleogenetic phase. Meso-morphologic features indicative of rising fluid-flow currents and buoyant convection circulation are abundant throughout the caves.

A substantial degree of hydrogeological confinement is a necessary condition for a forced ascending groundwater circulation to occur. The morphogenetic analysis suggests that the whole cave system developed in a rather uniform pressure field, which implies a considerable degree of confinement of the flow system. If the system were not confined enough, speleogenetic competition (the positive feedback between flow and conduit growth) would determine the development of a few prominent sub-vertical conduits rather than a laterally distributed system. The considerable degree of confinement, in turn, implies that cave development has occurred at considerable depth, because necessary confinement by the Salitre Formation itself could not be provided in a comparatively shallow position. Moreover, it is likely that a major confining unit above carbonates existed during the main speleogenetic phase, comprised of insoluble rocks of low permeability. This is suggested by the occurrence of morphologically similar outlets in groups, such as two pairs of outlets in Sector C and a cluster of rift-like outlets in Sector D (see Section 6.3 and Fig. 16). The uniform development of several outflow paths across a major hydrostratigraphic barrier in the same area was possible only if an external conservative control over discharge in the whole rising flow system is provided by some low-permeable overlying unit to suppress the positive flow-dissolution feedback (Klimchouk, 2007, 2014).

The TBV and TBR passages form elongated fields, together constituting a "cave corridor" that stretches NE-SW (Fig. 2B). It represents speleogenetically exploited, large fracture corridor, which exactly follows the line of a major thrust that extends to SW of the caves for almost 100 km, disrupting Mesoproterosoic sediments (Fig. 2A). Fracture corridors or swarms (localized arrays of fractures within a discrete volume of the rock characterized by greater fracture density than its surrounds; Ogata et al., 2014) are increasingly recognized as major controls of fluid flow in sedimentary sequences (Singh et al., 2008; Bush, 2010; Questaux et al., 2010; Ogata et al., 2014). As the rocks that underlie the Salitre carbonates in the area do not form a diffuse-flow aquifer, formation of the TBV-TBR system relied upon flow rising from greater depths to the bottom of the Salitre carbonates along the regional thrust. The chief determinant of the localization and overall configuration of the TBV-TBR system was that the fracture corridor in the hanging wall of the thrust provided a zone for the deep fluid flow to rise across the Salitre carbonates.

Within the fracture corridor of generally enhanced vertical permeability, hydrostratigraphy and patterns of transverse fluid flow depend on variations in fracture density and aperture between units and, rather critically, on the vertical connectivity of the fracture networks. The lack of vertical connectivity between fractures, limited to or contained within specific lithostratigraphic units (horizons), creates interfaces impeding vertical flow even in otherwise lithologically uniform sequences (Klimchouk, 2000, 2007; Underwood et al., 2003; Eaton, 2006). Breaches in such interfaces

determine the pattern of recharge for units immediately above the interfaces. Large, vertically extensive fractures that cross boundaries of units are particularly important for vertical flow.

In the TBV-TBR system, recharge from below occurred via near-vertical fractures of predominantly NE-SW to NNE-SSW orientation in the lower cave stratigraphic storey (Unit 1). Most of large fractures in Unit 1 terminate in its upper part, that creates the first hydrostratigraphic interface, an imperfect barrier to vertical flow. Those fractures that occasionally penetrated upward into units 3-4, as well as connecting to combinations of smaller fractures in units 2-3, provided outlets for flow to reach the laterally conductive horizon of Unit 4. In Unit 4, flow was redirected laterally because of a combination of the following factors: 1) high original (pre-speleogenetic) lateral permeability of this unit due to thinner bedding and dense fracturing, 2) very low fracture density in the basal part of Unit 5, and 3) strong discordance (mismatch in the plan view) of patterns between recharge features in Unit 1 and discharge features in Unit 5. Factors 2 and 3 caused the second and the most expressed hydrostratigraphic interface at the bottom of Unit 5, acting as a seal hindering rising flow and redirecting it laterally. Most lateral flow in Unit 4 was conducted along the hinges of anticlines where fracture density was the greatest. The outflow paths from the main karstified interval were established where the integrity of the major seal was breached by large sub-vertical fractures in the basal part of Unit 5, connected with other conducting fractures in still upper parts of the sequence (units 6-7).

In the overall ascending flow system, the formation of the cave pattern was controlled by specific structural conditions (gentle folding) and vertical (fracture stratigraphy) and lateral heterogeneities in fracture distribution.

6.3 Functional organization of the cave system

The gross three-dimensional pattern of the system is organized to effectively convey rising flow in deep-seated confined conditions, under given geological constraints (Figs. 9, 10, 16). Individual sub-vertical feeders and their merged clusters at the lower cave stratigraphy storey (in Unit 1) served as points and areas of ascending recharge to the system. Termination of many sub-vertical fractures of the lower storey at the top of Unit 1 caused that many cave clusters at this storey are separated from passages at the next storey above, connecting to them only by few conduits (Figs. 10, 12).

The laterally extensive conduit network at the middle cave-stratigraphy storey functioned to collect the rising flow from numerous individual recharge points and areas to master passages of the dominant N-S and NE-SW orientation formed along crests of anticlines, and to further distribute flow toward outlet structures.

Rift-like and shaft-like conduits at the upper storey developed along fracture-controlled outflow paths breaching the integrity of the major seal. The rift-type morphology is also characteristic of passages in the upper part of Unit 7 observed in the nearby cliff and the quarry, which are analogues of the outflow subsystem that once existed above the TBV-TBR cave system but have been denuded away.

The main map in Fig. 16 shows distribution of major recharge and discharge components in TBV. Only large recharge areas (coalesced chambers and passage clusters at the lower storey; indicated in pink color) and most prominent individual feeders (indicated as red circles) are shown in the map. Thousands of smaller side feeders (photos D-L in Fig. 13) are scattered throughout the passage network at the middle storey, like those mapped along the master passage a2 in the upper left inset (small dots). It can be seen that major recharge components tend to concentrate along the NW border of the cave, likely indicating the location of main fluid-supplying disruptions in rock that underlie the Salitre Formation.

The main function of the passage network at the middle storey was to collect rising flow from numerous individual recharge points and areas to the master conduits formed along hinges of anticlines, and to further distribute flow toward the outlet structures. This is well illustrated by morphogenetic mapping in area 3 (upper left inset in Fig. 16), where the master passages at hinges of anticlines (a1, a2 and a3) drained adjacent smaller conduits that collected recharge from below, and conducted more concentrated flow to the nearest outlets breaching the integrity of the major seal (two in a1 passage and two in a3 passage). It is possible to distinguish individual drainage areas, within which lateral flow directions differ (Fig. 16, upper left inset).

Major outlets that provided discharge up from the main cave interval are scarce (Fig. 16). Four individual outlets are found in Sector B, two in Sector E, and a cluster of rift-like outlets occurs in Sector D (the "discharge area" enclosed by the green dotted line in Fig. 16). Some additional unidentified outlets may exist. It is likely that outlets existed near the main entrance in sector A. In any case, hampering of vertical flow by the seal at the bottom of unit 5 is obvious.

TBV represents, in fact, a series of vertically organized, functionally largely independent three-dimensional clusters of cavities, developed within individual ascending flow cells. Lateral integration of clusters occurred due to hydrodynamic interaction between these flow cells along the laterally conductive Unit 4 below the seal (the bottom of Unit 5) in the course of speleogenetic evolution and change of boundary conditions. In contrast, TBR represents a large cluster of lower-storey cavities comprising a number of smaller clusters, lateral integration of which at this storey was forced by the absence of laterally conductive Unit 4 and breaches in the overlying seal (the bottom of Unit 5) across

a large area. Discharge from this cluster likely occurred via unmapped parts of the system to NE (where the present-day entrance is located) and to SW (toward TBV) of the TBR area.

6.4 Speleogenetic phases

It is possible to identify at least three major speleogenetic phases for the TBV-TBR system.

The early phase. There are indications for at least two speleogenetic events that pre-date the main speleogenetic phase. One is evidenced by the presence of cavities in the upper part of unit 7 surrounded by the fluid-induced alteration halo (Fig. 6D). The halo is also developed around bedding planes and joints. This suggests that these cavities existed before alteration occurred or were formed during the same fluid event that caused alteration. The conduits of the main system lack this alteration halo and, therefore, they were formed after this event.

Another early event could have produced the cavities now represented by irregular meter-scale bodies of breccia that were completely destroyed before the onset of the main speleogenetic phase (Fig. 7). These bodies are intersected by the dissolution surface of the main cavities, indicating that the breccia pre-dates the main speleogenetic phase.

The main phase. The main phase was the development of the cave system with the pattern observed today, organized to effectively conduct rising flow in deep-seated confined conditions. In the upwelling flow system, the formation of the three-dimensional pattern of the caves was controlled by lateral and vertical heterogeneity in distribution of flow-conducting fractures, and by the pattern of fold axes. During this phase the gross cave pattern was established and the caves acquired most of their volume.

The latest phases. There was a distinct phase of water-table and subaerial development, when the water table has been positioned, possibly in several distinct episodes, at the hypsometric level intersecting at least some cavities at the lower stratigraphic storey of the cave system. This is suggested by the wide occurrence of watertable-related and shallow subaqueous speleothems (calcite coralloids, coatings, rafts, shelfstone). U-series dating of these speleothems yielded at least two periods of watertable rise at TBV, one centered between 17.3 – 20.1 ka, and another at ca. 144 ka (Auler and Smart, 2001). Above the watertable, some modification of morphology occurred due to condensation corrosion and subaerial dolomite weathering (Auler and Smart, 2004). Abundant and diverse sediments and speleothems that accumulated during the latest phases record a complex hydrogeologic, geomorphologic and climatic history during this phase, which is the subject of ongoing studies.

6.5 The regional geodynamic context of hypogene speleogenesis

The above presented analysis suggests that the main phase of TBV-TBR speleogenesis occurred in confined deep-seated settings due to fluid rise along the regional thrust and associated ruptures. Hypogene speleogenesis of this type commonly occurs during tectonic/geodynamic events that facilitate and or drive ascending fluid migration (Klimchouk, 2012, 2013). The timing of the main speleogenetic phase and the nature of the cave-forming flow system can be tentatively identified by analysis of the regional geodynamic evolution.

A sequence of geodynamic and tectonothermal events that occurred from ca. 600 to 510 Ma in the African continental area and adjacent Gondwana terranes are broadly referred to as the Pan-African Cycle, or the Brasiliano Cycle in South America (Teixeira et al., 2007). The Brasiliano orogeny affected the terranes of the present South American continent to the east of the Andes cordillera. The last period of deformations (540–500 Ma) was characterized by fissure magmatism and hydrothermal events along faults. However, a few cratons, including the São Francisco craton, were only weakly deformed by this event (Almeida et al., 2000).

Among the major stages of evolution of the São Francisco Craton that took place after accumulation of the Salitre Formation, the Cambrian tectonothermal event at about 520 Ma could be of special relevance for hypogene speleogenesis. This event was marked by large-scale remagnetization and resetting of the U–Pb isotopic system (Trindade et al., 2004). The most common mechanism responsible for such widespread remagnetization is the interaction of sediments with fluids expelled or derived from orogenic belts at the borders of cratonic areas (Oliver, 1986; Garven, 1995).

Trindade et al. (2004) attributed resetting of isotopic and magnetic systems in the Neoproterozoic sediments to the large-scale fluid migration and mineralization across the craton in the aftermath of the Brasiliano orogeny, driven by several interacting mechanisms: 1) tectonic deformation at the orogenic fronts that expelled reactive fluids towards the basin, 2) high hydraulic head provided by the surrounding mountain chains, that could drive deep regional flow of brines across the craton, and 3) deep fluids rising from the basement.

Hydrothermal fluids that raised from the basement and migrated by structurally controlled channelways during Cambrian tectonic re-activation, were responsible for the widespread sulphide (galena and pyrite) and other mineralizations hosted by the Salitre carbonates (Silva et al., 2006; Teixeira et al., 2010). Studies of fluid inclusions in sphalerite from Pb-Zn yielded mean formation temperatures for various locations ranging between $138^{o} – 185^{o}C$. The fluids were mainly NaCl brines.

In sphalerite inclusions from the Irecê deposits, closest to our study area, homogenization temperatures vary between 140 and 200°C (Teixeira et al., 2010).

Although the emplacement of this mineralization obviously post-dates the host rocks, they present radiogenic Pb signatures yielding an apparent Pb-Pb isochron age of 2138 ± 49 Ma (Toulkeridis et al., 1999; Misi, 1999). Anomalous Archean to Paleoproterozoic Pb signatures are also observed in sulfide mineralization (Iyer et al., 1992) and the host carbonates of the southern part of the basin (Babinski et al., 1999). Based on the analysis of Pb isotopic data of non-radiogenic and radiogenic (old) crustal Pb for these carbonates, Trindade et al. (2004) suggested that the ages of 520 and 2100 Ma track the Pb evolution that took place in the basement until its introduction into the Neoproterozoic carbonates at 520 Ma. They concluded that the similarity of the Pb signatures in both carbonates and sulfides indicates a common source for the fluids responsible for the Pb–Zn mineralization and remagnetization of the carbonates, i.e. the mineralization and remagnetization events overlapped in time at about 520 Ma. We suggest that this Cambrian fluid-flow event could also be responsible for the main phase of hypogene speleogenesis in the Campo Formoso area and the wider region.

Another important tectonic event was the Pangea break-up, which occurred from the end of the Triassic until later Cretaceous, during the Atlantic opening. This breakup generated several basins associated with mafic magmatism along the eastern margin of the South American continent, including the Tucano rift basin (Almeida et al., 2000), east of our study area (Fig. 1). The Tucano basin was generated by several NW- to NE-striking faults, most of which represent the reactivation of Precambrian ductile shear zones (Magnavita, 1994), mainly during Neocomian-early Barremian times (Matos, 1992). Several studies point to multiple phases of burial and denudation in the São Francisco craton and its surrounding fold belts since the Early Cretaceous break-up (Magnavita et al., 1994; Nóbrega et al., 2005; Morais Neto et al., 2009; Japsen et al., 2012). Thus, rifting associated with the Pangea break-up (Triassic – Cretaceous) and related geodynamic/fluid history events are another possible drivers for the main phase of deep-seated hypogene speleogenesis that created the TBV-TBR system.

The established oldest caves so far are Jenolan Caves in the Late Silurian limestones in the eastern Australia, where unlithified clay deposits yielded K-Ar age at 340 Ma (Early Carboniferous; Osborne et al., 2006). The second inferred option for the timing of TBV-TBR speleogenesis would place these caves among the oldest large studied caves in the world, and the first option implies that they could be the oldest ones. The speleogenetic analysis suggests that the main phase of their development occurred at considerable depth, likely around or greater than one km. The conditions of

preservation of these caves through geologically long periods may include: slow development of conduits and voids (which prevented significant stress buildup), likely over-pressurization of cave-forming fluids during the formation period (which partly compensated for the overburden load), balanced and low-to-moderate rates of uplift and denudation since at least Miocene (which resulted in gradual stress release), high strength of rocks comprising the Neoproterozoic Salitre succession (particularly of the Unit 5 bridging over the main cave storey), and generally low tectonic activity in this part of the craton since the main speleogenetic phase. The latter is evidenced by the fact that no clear post-speleogenetic tectonic deformations were identified in the caves.

Conclusions

Integration of detailed speleomorphogenetic studies and studies of lithostratigraphy and geological structure has allowed us to unravel the origin of the large TBV-TBR cave system in the Neoproterozoic carbonates of NE Brazil and to reveal its functional organization and geologic controls over the cave development. The caves were formed under deep-seated, confined conditions by rising deep flow, i.e. the caves are of the "true" hypogenic origin in the sense of the hydrogeological notion of hypogenic speleogenesis.

The localization of the cave system is determined by specific structural conditions permitting an access of deep fluids to the bottom of the Salitre Formation and rising flow across it, namely by the presence of a large NE-SW-trending fracture corridor associated with the major thrust disrupting the underlying rocks. The cave-forming fluid flow and hence the development of the TBV-TBR cave system were strongly controlled by fractures which distribution was influenced by lithostratigraphy (mechanical stratigraphy) and folding. The three cave-stratigraphic storeys identified in the cave system reflect the actual hydrostratigraphy during the main phase of speleogenesis. Cavities in the different storeys are distinct in morphology and functioning.

The gross three-dimensional pattern of the system is effectively organized to conduct rising flow in deep-seated confined conditions under the given geological constraints. The cave system represents a series of vertically organized, functionally independent clusters of cavities developed within individual ascending flow cells. Integration of clusters and the formation of laterally extensive conduit networks in the middle storey occurred along the laterally conductive unit (Unit 4), which lies below the unit of low vertical permeability (Unit 5). The latter hampered the vertical flow and served as an imperfect seal.

At least three distinct speleogenetic phases are identified. Some episodes of the early phase could have been related to upwelling of hypogene fluids through freshly deposited carbonates on the

sea bottom. During the main phase, the gross cave pattern was established to conduct rising flow in deep-seated confined conditions, and the caves acquired most of their volume. The timing of this phase cannot be constrained with confidence but it was likely related to the rise of deep fluids at about 520 Ma, which is thought to be responsible for large-scale remagnetization, resetting of the U–Pb isotopic system, and emplacement of the Pb-Zn mineralization across the São Francisco Craton. An alternative possibility is that the geodynamic/fluid history events associated with rifting and the Pangea break-up in the Triassic–Cretaceous were responsible for the main phase of deep-seated hypogenic speleogenesis that created the TBV-TBR system.

This study illustrates that patterns and functioning of deep-seated hypogene karst systems differ fundamentally from systems originated in surface-related epigene karst settings. It highlights the efficiency of the cave stratigraphy and functional organization approaches in studying hypogene speleogenesis in stratigraphically varied, fractured sequences. It also highlights the paramount importance of determination of the origin of solution void-conduit systems for understanding the highly heterogeneous distribution of porosity, permeability and flow in carbonate reservoirs, which presents one of the major challenges in prospecting and developing hydrocarbon resources.

Acknowledgements

References

Almeida, F.F.M., Brito Neves, B.B., Carneiro, C.D.R., 2000. The origin and evolution of the South American Platform. Earth Science Reviews 50, 77-111.

Audra, P. Mocochain, L., Bigot, J.-Y., Nobécourt, J.-C., 2009a. Morphological indicators of speleogenesis: hypogenic speleogenesis, in: Klimchouk, A., Ford, D. (Eds.), Hypogene speleogenesis and karst hydrogeology of artesian basins. Ukrainian Institute of Speleology and Karstology, Simferopol, pp. 17-22.

Audra, P., Mocochain, L., Bigot, J. Y. & J.C.Nobecourt, 2009b: Hypogene cave patterns, in: Klimchouk, A., Ford, D. (Eds.), Hypogene speleogenesis and karst hydrogeology of artesian basins. Ukrainian Institute of Speleology and Karstology, Simferopol, pp. 23–32.

Auler, A.S., 1999. Karst Evolution and Palaeoclimate of Eastern Brazil. PhD Thesis, University of Bristol.

Auler, A.S., Smart, P.L., 2001. Late quaternary paleoclimate in semiarid northeastern Brazil from U-series dating of travertine and water-table speleothems. Quaternary Research 55, 159–167.

Auler, A.S., Smart, P.L., 2003. The influence of bedrock-derived acidity in the development of surface and underground karst: evidence from the Precambrian carbonates of semi-arid Northeastern Brazil. Earth Surf. Process. and Landforms 28, 157-168.

Auler, A.S., Smart, P.L., 2004. Rates of condensation corrosion in speleothems of semi-arid northeastern Brazil. Speleogenesis and Evolution of Karst Aquifers 2, 2.

Babinski, M., Van Schmus, W.R., Chemale Jr., F., 1999. Pb–Pb dating and Pb isotopic geochemistry of Neoproterozoic carbonate rocks from the São Francisco basin, Brazil: implications for the mobility of Pb isotopes during tectonism and metamorphism. Chem. Geol. 160, 175–199.

Birmingham A.N., Mylroie J.R., Mylroie J.E., Lace, M.J., 2011. Bell hole origin: constraints on developmental mechanisms, Crooked Island, Bahamas. Speleogenesis and Evolution of Karst Aquifers, 11.

Bizzi, L. A., Schobbenhaus, C., Vidotti, R. M., Gonçalves, J.H., 2003. Geologia, Tectônica e Recursos Minerais do Brasil. Texto, Mapas e SIG. CPRM – Serviço Geológico do Brasil, Brasília.

Bögli, A., 1980. Karst hydrology and physical speleology. Springer-Verlag, Berlin.

Bristow, T.G., Bonifacie, M, Derkowski, A, Eiler, J.M, Grotzinger, J.P., 2011. A hydrothermal origin for isotopically anomalous cap dolostone cements from south China. Nature 474, 68-71, doi:10.1038/nature10096

Brito Neves, B. B., Fuck, R.A., Martins, M., 2014. The Brasiliano collage in South America: a review. Brazilian Journal of Geology 44, 493–518.

Bush, I. 2010. An Integrated approach to fracture characterization. Oil Review Middle East 2, 88- 91.

Cazarin, C.L., Bezerra, F.H.R., Borghi, L., Soares, J.A., Klimchouk, A., Balsamo, F., Auler, A., Machado, A.S., 2015. Facies control on hypogenic karst system in Neoproterozoic carbonates in Brazil. Geologia USP. Série Científica. Submitted.

Dublyansky, Y.V., Klimchouk, A.B., Spötl, C., Timokhina, E.I., Amelichev, G.N., 2014. Isotope wallrock alteration associated with hypogene karst of the Crimean Piedmont, Ukraine. Chem. Geol. 377, 31-44.

Dublyansky, Y., Spötl, C., 2015. Condensation-corrosion speleogenesis above a carbonate-saturated aquifer: Devils Hole Ridge, Nevada. Geomorphology 229, 17-29.

Eaton, T.T. 2006. On the importance of geological heterogeneity for flow simulation. Sedimentary Geology 184, 187–201.

Ford, D.C., Williams, P.W., 1989. Karst geomorphology and hydrology. Unwin Hyman, London.

Ford, D.C., Williams, P.W., 2007. Karst Hydrogeology and Geomorphology. Wiley, Chichester.

Garven, G., 1995. Continental-scale groundwater flow and geologic processes. Annu. Rev. Earth Planet. Sci. 23, 89–117.

Iyer, S.S., Hoefs, J., Krouse, H.R., 1992. Sulfur and lead geochemistry of galenas from the Bambuí Group, Minas Gerais, Brazil - implications for the ore genesis. Econ. Geol. 87, 437–443.

Japsen, P., Bonow, J.M., Green, P. F., Cobbold, P.R., Chiossi, D., Lilletveit, R., Magnavita, L.P., Pedreira, A.J., 2012. Episodic burial and exhumation history of NE Brazil after opening of the South Atlantic. GSA Bulletin 124, 800-816, doi: 10.1130/B30515.1

Klimchouk, A.B., 2000. Speleogenesis under deep-seated and confined settings, in: Klimchouk, A., Palmer, A., Ford, D., Dreybrodt, W. (Eds.), Speleogenesis: Evolution of Karst Aquifers. National Speleological Society, Huntsville, Al., pp. 244-260.

Klimchouk, A.B., 2007. Hypogene Speleogenesis: Hydrogeological and Morphogenetic Perspective. National Cave and Karst Research Institute, Carlsbad.

Klimchouk, A.B., 2009. Morphogenesis of hypogenic caves. Geomorphology 106. 100-117.

Klimchouk, A.B., 2012. Speleogenesis, Hypogenic, in: White, W.B., Culver, D.C. (Eds.), Encyclopedia of Caves, 2nd edition, Elsevier, Academic Press, Chennai, pp. 748-765.

Klimchouk, A.B., 2013. Hypogene speleogenesis, its hydrogeological significance and the role in evolution of karst. DIP, Simferopol (in Russian).

Klimchouk A.B., 2014. The methodological strength of the hydrogeological approach to distinguishing hypogene speleogenesis, in: Klimchouk, A., Sasowsky, I., Mylroie, J., Engel, S.A., Engel, A.S. (Eds.), Hypogene Cave Morphologies. Karst Waters Institute, Leesburg, Virginia, pp. 4-12.

Klimchouk, A.B., Ford, D.C. (Eds), 2009. Hypogene Speleogenesis and Karst Hydrogeology of Artesian Basins. Ukrainian Institute of Speleology and Karstology, Simferopol, 280 p.

Klimchouk, A., Ford, D.C., Palmer, A.N., Dreybrodt, W. (Eds.), 2000. Speleogenesis: Evolution of karst aquifers. National Speleological Society, Huntsville, Al., 527 p.

Lauritzen, S.-E., Lundberg, J., 2000. Solutional and erosional morphology of caves, in: Klimchouk, A., Palmer, A., Ford, D., Dreybrodt, W. (Eds.), Speleogenesis: Evolution of Karst Aquifers. National Speleological Society, Huntsville, Al., pp. 408-426.

Magnavita, L.P., Davison, I., Kusznir, N.J., 1994. Rifting, erosion, and uplift history of the Recôncavo-Tucano-Jatobá Rift, northeast Brazil. Tectonics 13, 367–388, doi:10.1029/93TC02941.

Matos, R.M.D., 1992. The northeast Brazilian rift system. Tectonics 11, 766-791.

Misi, A. 1993. A Sedimentação Carbonática do Proterozóico Superior no Cráton do São Francisco: Evolução Diagenética e Estratigrafia Isotópica. II Symposium on the São Francisco Craton. Salvador, Brazil, Extended abstracts, p. 192-193.

Misi, A., 1999. Um modelo de evolução metalogenética para os depósitos de zinco e chumbo hospedados em sedimentos proterozóicos de cobertura do Cráton do São Francisco (Bahia e Minas Gerais). Unpublished Full Professorship Thesis. UFBA, Brazil, 151 p.

Misi, A., Kaufman, A.J., Veizer, J., Powis, K., Azmy, K., Boggiani, P. C., Gaucher, C., Teixeira, J.B.G., Sanches, A.L., Iyer, S.S., 2007. Chemostratigraphic correlation of Neoproterozoic successions in South America. Chem. Geol. 237, 22-45., doi:10.1016/j.chemgeo.2006.06.019.

Misi, A., Kyle, J.R., 1994. Upper Proterozoic carbonate stratigraphy, diagenesis, and stromatolitic phosphorite formation, Irecê Basin, Bahia, Brazil. Journal of Sedimentary Research A64, 299-310.

Misi, A., Veizer, J., 1998. Neoproterozoic carbonate sequences of the Una Group, Irece Basin, Brazil: chemostratigraphy, age and correlations. Precambrian Research 89, 87-100.

Montaron, B. 2008. Confronting carbonates. Oil Review Middle East 5, 132-135.

Morais Neto, J.M., Hegarty, K.A., Karner, G.D., Alkmim , F.F., 2009. Timing and mechanisms for the generation and modification of the anomalous topography of the Borborema Province, northeastern Brazil. Marine and Petroleum Geology 26, 7, 1070-1086, doi:10.1016/j.marpetgeo.2008.07.002.

Nóbrega, M.A., Sá, J.M., Bezerra, F.H.R., Hadler Neto, J.C., Iunes, P.J., Guedes, S., Tello Saenz, C.A., Hackspacher, P.C., Lima-Filho, F.P., 2005. The use of apatite fission track thermochronology to constrain fault movements and sedimentary basin evolution in northeastern Brazil. Radiation Measurements 39, 627-633.

Ogata, K., Senger, K., Braathen, A., Tveranger, J., 2014. Fracture corridors as seal-bypass systems in siliciclastic reservoir-cap rock successions: Field-based insights from the Jurassic Entrada Formation (SE Utah, USA). Journal of Structural Geology 66, p. 162-187.

Oliver, J., 1986. Fluids expelled tectonically from orogenic belts: their role in hydrocarbon migration and other geologic phenomena. Geology 14, 99-102.

Osborne, R.A.L., 2007. Cathedral Cave, Wellington Cave, New South Wales, Australia. A multiphase, non-fluvial cave. Earth Surface Processes and Landforms 32, 2075-2103.

Osborne, R.A.L., Zwingmann, H., Pogson, R.E., Colchester, D.M, 2006. Carboniferous Cave Deposits from Jenolan Caves, New South Wales, Australia. Australian Journal of Earth Sciences 53, 3, 377-405.

Palmer, A.N., 2000. Hydrogeologic control of cave patterns, in: Klimchouk, A., Palmer, A., Ford, D., Dreybrodt, W. (Eds.), Speleogenesis: Evolution of Karst Aquifers. National Speleological Society, Huntsville, Al., pp. 77-90.

Palmer, A.N., 2007. Cave Geology. Cave Books, Dayton.

Penha, A.E.P.P., 1994. O calcário Caatinga de Ourolândia, Bahia: Feições diagnósticas, gênese e evolução de um perfil calcrete. MSc Dissertation, Universidade Federal da Bahia.

Questiaux, J.-M., Couples, G.D., Nicolas, R., 2010. Fractured reservoirs with fracture corridors. Geophysical Prospecting 58, 279–295.

Santos, R.V., Alvarenga, C.J.S., Dardenne, M.A., Sial, A.N., Ferreira, V.P., 2000. Carbon and oxygen isotope profiles across Meso-Neoproterozoic limestones from central Brazil: Bambuí and Paranoá groups. Precambrian Research 104, 107–122.

Shields, G.A., 2005. Neoproterozoic cap carbonates: a critical appraisal of existing models and the plume world hypothesis. Terra Nova 17, 299-310.

Silva, M.G., Neves, J.P., Klein, E., Bento, R.V., Dias, V.M., 2006. Principais processos envolvidos na gênese das mineralizações de Sn, Au, Ba, quartzo rutilado e diamante, na região do Espinhaço-Chapada Diamantina, Bahia. XLIII Congresso Brasileiro de Geologia, 2006, Aracaju. Anais do XLIII Congresso Brasileiro de Geologia, p. 161.

Singh, S.K., Abu-Habbiel, H., Khan, B., Akbar, M., Etchecopar, A., Montaron, B., 2008. Mapping fracture corridors in naturally fractured reservoirs: an example from Middle East carbonates. First Break 26, 5, 109-113.

Spötl, C., Pitman, J. K., 1998. Saddle (baroque) dolomite in carbonates and sandstones: A Reappraisal of a Burial-Diagenetic Concept., In: S. Morad (Ed.), Carbonate Cementation in Sandstones: Distribution Patterns and Geochemical Evolution. Blackwell Publishing Ltd., Oxford, UK, doi: 10.1002/9781444304893.ch19.

Spötl, C., Vennemann, T.W., 2003. Continuous-flow isotope ratio mass spectrometric analysis of carbonate minerals. Rapid Commun. Mass Spectrom. 17, 1004-1006.

Stafford, K., Land, L., & G. Veni (Eds.), 2009. Advances in Hypogene Karst Studies. National Cave and Karst Research Institute, Carlsbad. 182 p.

Suguio, K., Barcelos, J.H., Matsui, E., 1980. Significados paleoclimáticos e paleoambientais das rochas calcárias da Formação Caatinga (BA) e do Grupo Bauru (MG/SP). Proceedings XXXI Brazilian Geological Congress, 1, 607-617, doi:10.1016/j.gr.2006.05.009

Teixeira, J. B. G., Misi, A., Silva, M.G., 2007. Supercontinent evolution and the Proterozoic metallogeny of South America. Gondwana Research 11, 346-361.

Teixeira, J.B.G., Silva, M.G., Misi, A., Cruz, S.C.P., Silva Sá, J.H., 2010. Geotectonic setting and metallogeny of the northern São Francisco craton, Bahia, Brazil. Journal of South American Earth Sciences 30, 71-83.

Torquato, J.R.F., Misi, A., 1977. Medidas isotópicas de carbono e oxigênio em carbonatos do Grupo Bambui na região centro-norte do Estado da Bahia. Revista Brasileira de Geociências 7, 14-24.

Toulkeridis, T., Misi, A., Todt, W., Gomes, A.S.R., Babinski, M., Buscwaldt, R., 1999. Early Proterozoic galenas from Neoproterozoic sulphides, Irecê basin, Bahia, Brazil. EUG Meeting 10, Strasbourg, France, Abstracts, p. 811.

Trindade, R.I.F., D'Agrella-Filho, M., Babinski, M., Neves, B.B., 2004. Paleomagnetism and geochronology of the Bebedouro cap carbonate: evidence for continental scale Cambrian remagnetization in the São Francisco Craton, Brazil. Precambrian Research 128, 83-103.

Underwood, C. A., M. L. Cooke, J. A. Simo, Muldoon, M.A., 2003, Stratigraphic controls on vertical fracture patterns in Silurian dolomite, northeastern Wisconsin. AAPG Bulletin 87 (1), 121-142.

van Golf-Racht, T., 1982. Fundamentals of fractured reservoir engineering. Elsevier, Amsterdam.

Appendix

The stratigraphic position of the cave-hosting carbonates

Determining a position for the cave-hosting sequence within the broader stratigraphic section sheds some light to possible depth of burial and is important for regional-scale correlations with other fluid-related phenomena in the Neoproterozoic carbonates of the São Francisco Craton. It is also necessary for interpretation of the observed variations in stable isotope composition with regard to chemostratigraphy established for the Salitre formation in the broader region (Torgato and Misi, 1977; Misi and Veizer, 1998; Misi et al., 2007).

A carbonate mega-sequence that occurs in the São Francisco, Irecê and Una-Utinga basins of the São Francisco Craton, including the Salitre Formation and its correlative units, preserves two shallowing-upward sub-sequences representing two transgressive–regressive marine cycles (Fig. A1; Misi et al., 2007). In the Irecê Basin, adjacent to the south of the Campo Formoso area, the Salitre Formation was subdivided informally, from the base to the top, into units C, B, B1, A and A1 (Fig. A1B; Misi and Kyle, 1994; Misi and Veizer, 1998; Misi et al., 2007). The lowermost Unit C, represented in the eastern portions of the Irecê Basin by red (pink) to green argillaceous dolomites (Misi and Veizer, 1998; Misi et al., 2007), is characterized by whole rock $\delta^{18}O$ values ranged from -5.3 to -10.7 ‰ and strongly negative values of $\delta^{13}C$ (ca. -6 ‰; Torguato and Misi, 1977). Carbonates that overlie Neoproterozoic glacial deposits worldwide are recognized as cap carbonates, whose deposition is thought to be associated with the flooding of continental shelves and platforms as the ice sheets melted. Negative $\delta^{13}C$ values are common for cap carbonates (Shields, 2005), and this characteristic depletion was deemed to be caused by the release of carbon from reservoirs formed by burial of dead organisms at the end of the Snowball Earth events and destabilization of gas hydrates in sea-floor sediments, with subsequent oxidation of methane to CO_2 in the atmosphere and acidification of the oceans. However, recent detailed isotope studies of Chinese cap carbonates suggest that the ^{13}C depletion can be related to permeation of the sediments by hydrothermal fluids that triggered oxidation of methane within the sediments themselves (Bristow et al., 2011). If this was the case with the Salitre carbonates, then these rising hydrothermal fluids could be responsible for the earliest phases of the hypogenic speleogenesis, some of which could have taken place in the sea-floor sediments soon after initial burial and consolidation.

Unit B of Misi and Veizer (1998) is characterized as parallel laminated gray limestone and dolomitic limestone. Unit B1 is represented by grey to red dolostone with teepee structures, intraformational breccia, calcite and silica nodules, cross and current-ripple bedding and laminated and columnar stromatolites (Misi et al., 2007). Dolomites of this unit bear phosphate and Zn-Pb

mineralization in the Irecê Basin and elsewhere in the São Francisco Craton. Unit A, present at the western border of the Irecê Basin but missing in its eastern part, is comprised of massive, organic-rich limestone with oolitic and pisolitic textures. It is characterized by strong ^{13}C enrichment with a mean value of +8.5 ‰ (Misi and Veizer, 1998; Misi et al., 2007).
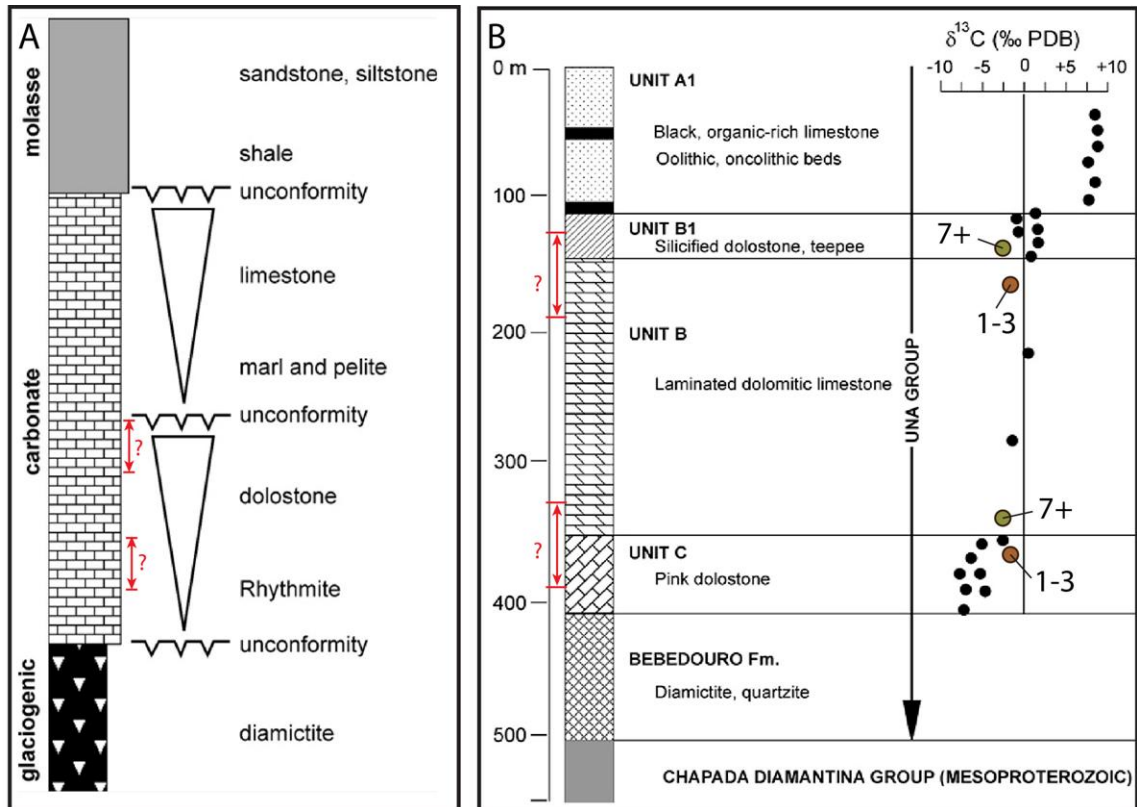

Figure A1. Lithostratigraphic position and division of carbonates of the Una Group, Irece Basin, stratigraphic variations of δ^{13}C (modified from Misi et al., 2007) and correlation of the cave-hosting sequence. A - Composite stratigraphic cartoon showing details of the three mega-sequences including the direction of shallowing and deepening in the two sub-cycles from the carbonate megasequence. B – stratigraphic variations of δ^{13}C in carbonates of the Una Group. Arrows approximate possible positions of the part of the sequence containing the TBV-TBR system. Large circles indicate average δ^{13}C values of different units from this study.

The above mentioned lithofacies and isotopic characteristics of Unit A definitely do not fit to those of the cave-hosting succession in the Campo Formoso area, so it is safe to conclude that there is no analogous unit there. Most of the facies features described for Unit B1 are observable in units 1-4 in the TBV-TBR area, as described in section 5.1. Based on this, the part of the Salitre Formation that contains the TBV-TBR system could be correlated with the upper part of Unit B and Unit B1 of the

Irecê Basin, as suggested by Auler (1999). In the more general stratigraphic cartoon in Fig. A1A, this rock package would correspond to the upper part of the older of the two shallowing-upward sub-sequences comprising the carbonate mega-sequence. However, δ^{13}C values measured in our samples are somewhat more depleted than those reported for units B1 and B in the Irecê Basin (Fig. A1B).

Alternatively, the cave-hosting succession can be correlated with the upper section of the unit C in the East Irecê Basin. Lithofacies characteristics of unit C given in the above cited works are too generalized (e.g. laminated argillaceous dolomites), and the two regions being compared are separated by several hundred kilometers so that an exact match is not expected. However, δ^{13}C values from our study match more closely to those reported for the upper part of unit C (Torgato and Misi, 1977; Misi and Veizer, 1998; Misi et al., 2007; see Fig. A1B). The main interval of cave development in the Campo Formoso area lays not far (ca. 100 m) from the lower contact of the Salitre Formation, which further supports this hypothesis. We conclude, therefore, that the cave-hosting succession is most likely correlative to the upper part of Unit C.